Tissue-Specific Influence on Developmental Modulation in Response to Phosphate Deprivation in *Arabidopsis thaliana* Roots

by

Heidi Mae Cederholm

University Program in Genetics and Genomics
Duke University

April 8, 2013

Approved:

_____
Philip Benfey, Supervisor

_____
David McClay

_____
Sally Kornbluth

_____
Meng Chen

Dissertation submitted in partial fulfillment of
the requirements for the degree of Doctor of Philosophy in the University Program in Genetics and Genomics in the Graduate School
of Duke University

2013

ABSTRACT

Tissue-Specific Influence on Developmental Modulation in Response to Phosphate Deprivation in *Arabidopsis thaliana* Roots
by

Heidi Mae Cederholm

University Program in Genetics and Genomics
Duke University

April 8, 2013

Approved:

_____
Philip Benfey, Supervisor

_____
David McClay

_____
Sally Kornbluth

_____
Meng Chen

An abstract of a dissertation submitted in partial fulfillment of
the requirements for the degree of Doctor of Philosophy in the University Program in Genetics and Genomics in the Graduate School
of Duke University

2013

Abstract

Roots are developmentally plastic and highly dependent on the immediate environment. By studying root responses to abiotic stress, we have identified novel regulators of developmental modulation. When roots are deprived of phosphate (P_i), developmental programs are modulated to slow primary root growth and expand surface area through emergence of root hairs. By focusing on exposure time-periods of less than two days, we have described very early changes to root development in response to this condition that may reveal new mechanisms of root hair specification and emergence. Also, using transcriptomic analyses with high spatial resolution, we identified a kinase that is specifically induced in root vascular tissue within three hours of exposure and acts to modulate aspects of root development in response to deprivation of P_i. These data suggest that individual tissues play unique roles in whole organ development, and that interpretation of P_i -deprivation responses may change as we develop methods with resolution necessary to understand these roles. Beyond P_i, we compared transcriptomic data for four additional stresses and identified a novel stress-responsive transcription factor that modulates expression of a cell expansion protein. This putative network connection demonstrates the value of using high-dimensional data for inference of regulatory relationships. Overall, we have combined "-omics" approaches with reverse genetics to identify novel developmental regulators and

described a phenotypic frame-work with resolution at which cellular mechanisms of Pi-deprivation response can be studied.

Dedication

For Mom and Dad, thank you for your steadfast support-you lit my way when I felt unsure about stepping beyond my comfort zone to follow my dreams.

Contents

List of Tables

List of Figures

Acknowledgements

Thanks to my mentor, Philip Benfey, for fostering an environment of collegiality and collaboration in the lab. By giving me the freedom to explore and somewhat define my project, to seek out collaborations, and to pursue opportunities for learning beyond the laboratory, you have greatly enriched my graduate experience.

I would also like to thank my original committee members, Sally Kornbluth, Dave McClay, and Tom Mitchell-Olds for helpful perspective and continued support and encouragement throughout these years. Thanks to my new committee member, Meng Chen, for his guidance over these last few months.

Thanks to my colleagues in the Benfey lab for helpful discussions. A special thanks to post-docs Ross Sozzani, Jaimie Van Norman, and Louisa Liberman for their willingness to discuss experimental design and troubleshooting. And thanks to our technician, Heather Belcher, for cell-sorting support. I'd like to acknowledge my collaborator Iulian Pruteanu for his statistical analyses and tireless efforts towards our shared project, which is presented in Chapter 4. Also, I had the pleasure of mentoring several talented undergraduate interns Aneitra Hoggard, Lizzeth Alarcon, Mary Cate Earnhardt, and Allie Stewart-thank you all for your efforts in support of this thesis.

Finally, thank you to my husband-to-be for support of my career and for all of

the weekends you willingly spent in lab with me. It felt so good to enjoy our weekends together, even when I needed to work.

Chapter 1. Introduction

At the "root" of this thesis work is an interest in discovering tissue-specific regulators of root development to demonstrate that genes activated in few tissues can modulate whole-organ development. To model this, we studied changes to root morphology in response to deprivation of phosphate (P_i) and other abiotic stresses. A unifying theme throughout each of three chapters describing novel findings is an effort to elucidate how plants change developmental programs to modulate aspects of root morphology in response to abiotic stress.

The introduction will begin with discussion of root development and patterning of pertinent tissues, highlight connections between abiotic stress and development, continue with a synthesis of the current understanding of root responses to P_i deprivation, and state the overall hypothesis of this work. Chapters 2-4 will each cover an introduction to experimental methods, a discussion of findings in the context of current understanding of biology, and a description of future directions. In Chapter 2, we set out to describe novel characteristics of root developmental modulation in response to P_i deprivation and followed up with expression analysis to identify regulators of morphology. In Chapter 3, we stepped back to explore transcriptomic data collected from tissue types at varying spatial resolution and identified a novel, tissue-specific kinase that controls root development in response to P_i deprivation. In chapter 4, we combined our high-resolution expression data with that of four other investigators

in the lab to identify novel genes, and the networks in which they operate, controlling aspects of abiotic stress response by analyzing high-dimensional data in an unbiased fashion. Chapter 5 will briefly discuss implications of this work and conclude the thesis. Overall, our studies have added to the understanding of genetic control of development and we have submitted these works for publication to the journal, The Plant Cell.

1.1 Primary root development

The simple structure and developmental pattern of the *Arabidopsis thaliana* root make it an ideal model for developmental biology. There are approximately 15 cell types in the root with the outer layers - the epidermis, cortex, and endodermis - arranged as a set of concentric cylinders that surround the central stele, or vascular tissue plus pericycle (Figures 1B and 1C; Benfey P and Scheres B, 2000). External to the epidermis, the lateral root cap and columella root cap protect the root tip as it moves through the soil. Each cell or tissue type in the root originates from a set of initials, akin to animal stem cells, located at the tip of the root in the stem cell niche (Figure 1B; Scheres B, 2007). Stem cells are maintained in an undifferentiated state by the quiescent center (QC), a set of mitotically less-active cells in the root tip. Plant stem cells, like animal stem cells, undergo asymmetric divisions resulting in a self-renewed initial cell and a daughter cell that can divide again. Daughter cells of each of the four sets of initials undergo different, but stereotyped, patterns of anticlinal division (plane of new cell wall is perpendicular to the root surface) and periclinal division (plane of new cell

wall is parallel to the root surface), resulting in the formation of all cell types within the root. Like animal cells, plant cell fate depends primarily on positional cues, rather than lineage.

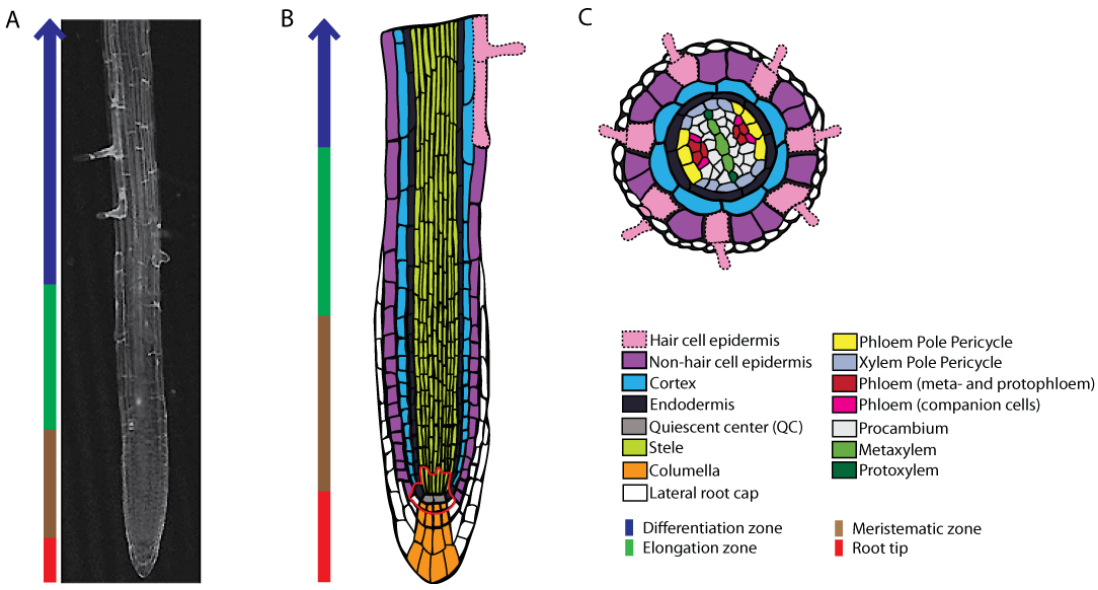

Figure 1: Root cell types and developmental zones. (A) Image of Arabidopsis thaliana root with developmental zones marked as colored line (blue = differentiation zone, green = elongation zone, brown = meristematic zone, red = root tip). (B) Schematic of longitudinal, median section showing tissue-types (see legend for color-scheme). Red outline marks the stem-cell niche. (C) Schematic of transverse section showing tissue-types.

Plant cells do not move in relation to one another, so each cell type is constrained in a file with position along the longitudinal axis of the root indicative of age. The youngest cells are found at the tip of the root in a transit amplifying, or rapid division, region termed the meristematic zone (MZ; Figures 1A and 1B). As distance from the stem cell niche increases, cells age and start to elongate. This begins the process of differentiation in the elongation zone (EZ; Figures 1A and 1B). Upon reaching full

maturity, cells enter the differentiation zone and take on specialized characteristics like root hairs in the epidermis (Figure 1A, 1B, and 1C). The balance between generation of new cells in the stem-cell niche and meristem and the cells leaving this zone to elongate determines the size of the root meristem (Dello Ioio et al., 2007; Dello Ioio et al., 2008; Moubayidin et al., 2010).

The last fifteen years have seen major advances in the understanding of root development with respect to genetic regulation. In particular, many transcriptional regulators controlling primary root patterning have been identified. Here, we describe roles for key regulators of development for tissues pertinent to our study. Other developmental influences include long-range hormone signaling and are discussed in the context of whole root development as opposed to individual tissues.

Vascular tissue

The central cylinder of tissue within the root consists of vascular tissue surrounded by pericycle cells. Collectively these tissues are referred to as the stele. Several cell types comprise this tissue, which is responsible for structural support and transport of water and nutrients throughout the plant. There are two phases of vascular development, termed primary and secondary. During primary development, vascular tissues consist of bundles of xylem and phloem tissues with surrounding procambial cells (Figure 1C). Secondary development occurs much later and involves vascular stem cell proliferation leading to radial growth and elaboration of vascular patterning. Xylem

cells at the center of the stele differentiate into metaxylem with reticulate or continuous cell wall thickenings and those at the periphery become protoxylem with annular or spiral walls. The role for mature xylem is to transport water and dissolved minerals from root to shoot. Phloem develops at two poles situated 90 degrees from the xylem-poles (Figure 1C) and contacts the phloem pole pericycle tissue. Phloem is responsible for transport of photosynthetic products like sugars, RNA, protein, and other organic compounds rootward. Here we discuss the known genetic regulators of xylem and phloem tissues and how development is influenced by hormones.

Vascular differentiation depends on proliferation of the procambial cells and is partially dependent on cytokinin signaling. WOODEN LEG (WOL), a histidine kinase, transduces cytokinin signals that may be required for proliferation. *wol* mutants have fewer vascular initial cells and end up specifying only protoxylem, indicating that WOL is required for formative divisions during embryogenesis as well as later for propagation of the vascular pattern (Mahonen et al., 2000). However, in a fass mutant background, which causes supernumary cell layers, *wol* exhibits markers for phloem development. These results indicate that WOL is not required for specification of phloem.

Although the mechanism is unknown, LONESOME HIGHWAY (LHW) is an additional regulator of vascular proliferation and differentiation. *lhw* mutants have fewer total vascular cells than wild type and specify a single strand of protoxylem

instead of two (Ohashi-Ito et al., 2007; Parizot et al., 2008). LHW encodes an atypical bHLH transcription factor that does not contain the canonical DNA-binding residues, but does localize to the nucleus and rescues the xylem pole phenotype when constitutively expressed. Normal expression of LHW is highest near the root meristem and seems to be enriched in the QC relative to other cell types (Ohashi-Ito et al., 2007). Taken together, these data suggest that LHW acts as a transcription cofactor to modulate expression of unknown regulators of protoxylem development. And although *wol* mutants have fewer vascular cells, multiple xylem poles are still specified in *wol lhw* double mutants, suggesting that *wol* is epistatic to *lhw* with respect to xylem cell identity.

The GRAS family transcription factors SHR and SCR play key roles in vascular development as well, although the roles are indirect. *scr* and *shr* mutants exhibit ectopic metaxylem in place of protoxylem in the stele, indicating that SCR and SHR are involved in xylem development and differentiation. This was shown to occur through a non-cell autonomous mechanism, as *SHR* transcript is produced in the vasculature, but SHR protein activates transcription of target genes, including SCR, in the endodermis (Helaruitta et al., 2000; Cui et al., 2007). To understand this mechanism, Carlsbecker et al. expressed SHR specifically in the ground tissue of shr-2 mutants, and were able to rescue protoxylem formation (Carlsbecker et al., 2010). This was not true of SHR expressed in the stele of these mutant plants. Additionally, SCR expression in the ground tissue in the shr mutant background could not rescue the protoxylem

phenotype, indicating that both SHR and SCR are required in the ground tissue for vascular specification of protoxylem (Nakajima et al., 2001). A genetic screen for vascular pattern defects revealed that *miR165a* and *miR166b* (miR165/6) restrict expression of the HD-ZIP class III transcription factor PHB primarily to the metaxylem precursors and procambial cells of the stele (Figures 5A and 5B). Previous work had shown that HD-ZIP III transcription factors also regulate vascular tissue proliferation (Prigge et al., 2005). Analysis of *shr-2 phb* double mutants indicated that correct xylem differentiation depends on the restriction of PHB transcripts to the center of the stele within the meristematic zone. This restriction is regulated by SHR activation of miR165/6 in the endodermis. Using ChIP-qPCR, the authors showed that SHR directly binds to regions upstream of the transcription start site for miR165b and miR166a. These results, together with data from reporter construct expression, strongly suggest that these microRNAs are activated by SHR and SCR within the endodermis, but then move to the vasculature to directly repress PHB transcript expression. Thus they regulate xylem differentiation non-cell autonomously. In addition, through analysis of quadruple and quintuple HD-ZIP III transcription factor mutants, Carlsbecker et al. showed that the expression levels of these transcription factors help determine xylem cell types (Carlsbecker et al., 2010).

Two additional transcription factors influencing xylem vessel formation in the root were identified using an inducible in vitro system. VASCULAR-RELATED NAC

DOMAIN 6 (VND6) and VND7 are NAC domain transcription factors that can induce metaxylem and protoxylem-like elements when overexpressed (Kubo et al., 2005; Yamaguchi et al., 2008; Yamaguchi et al., 2010). Constitutive repression of VND6 target genes resulted in repression of metaxylem formation, however normal protoxylem vessel formation was observed, suggesting that VND6 normally promotes metaxylem formation. In contrast, constitutive expression of a VND7 repressor led to repression of protoxylem formation, but normal metaxylem formation occurred, suggesting that VND7 normally functions to promote protoxylem fate. Interestingly, knock-down lines of VND6 or VND7 by T-DNA insertion or RNAi showed no vessel morphology defects, indicating the presence of functionally redundant genes.

Cytokinin signalling through WOL and other cytokinin-binding receptor proteins is required for proliferation and/or maintenance of procambium. By inducing expression of CYTOKININ OXIDASE 1, Mahonen et al. depleted wild type plants of cytokinin post-embryonically, and showed that all vascular cells became protoxylem (Mahonen et al., 2006). Therefore cytokinin is required to develop or maintain other vascular fates, like metaxylem. To identify genes controlling cytokinin-induced vascular morphogenesis, the authors conducted a suppressor screen in the *wol* background. One of these suppressors, ARABIDOPSIS HISTIDINE PHOSPHOTRANSFER PROTEIN 6 (AHP6) was found to promote protoxylem identity, as *ahp6* mutants exhibited defects in protoxylem differentiation. Additionally, *wol ahp6* double mutants have more vascular

cell files, including procambium and phloem cells. The AHP6 expression domain is constrained by cytokinin, which in turn is repressed by AHP6. These data suggest that a balance between cytokinin signalling and its inhibitor AHP6 maintains procambial cell identity and promotes differentiation to the protoxylem fate.

Cytokinin transport through the phloem is also important for maintaining vascular patterning. Cytokinin accumulates in the root tip, and is transported rootward through the phloem (Bishopp et al., 2011a). Specifically depleting cytokinin from the phloem led to defects in protoxylem differentiation. Grafting experiments suggested that this cytokinin was shoot-derived. Interestingly, depleting cytokinin from the phloem had no effect on meristem size, suggesting that rootward cytokinin transport in the phloem acts differently from the cytokinin network that controls meristem size. The authors suggested that cytokinin flow through the phloem allows targeting of specific pathways like vascular patterning, while not impeding other cytokinin regulated developmental pathways that may rely on locally produced cytokinin.

In addition to cytokinin, auxin is important for specifying the vascular pattern. Bishopp et al. showed that there are two domains of high hormonal response in the vasculature: high auxin in the xylem axis and high cytokinin in the procambial cells adjacent to the xylem axis (i.e. between the phloem and xylem; Bishopp et al., 2011b). Not only does cytokinin regulate expression of the PIN polar auxin transporters (Dello Ioio et al., 2008; Ruzicka et al., 2009), but high levels of cytokinin in the procambial cells

help to correctly position PIN1, PIN3 and PIN7. Auxin is then laterally distributed into the xylem axis, where it promotes expression of the cytokinin signaling inhibitor AHP6, thereby reinforcing the auxin maxima, and promoting protoxylem differentiation in a bisymmetric pattern. Blocking auxin transport resulted in loss of the auxin signaling maximum and loss of protoxylem identity. These data are consistent with the fact that strong mutations in either cytokinin or auxin signaling lead to vasculature containing only protoxylem (severe cytokinin mutants) or no protoxylem (severe auxin signaling mutants; Bishopp et al., 2008).

In addition to the many regulators known to specify xylem, one vascular regulator has been shown to be specifically required for phloem differentiation. ALTERED PHLOEM DEVELOPMENT (APL) encodes a MYB-coiled-coil type transcription factor that is required for the asymmetric divisions and subsequent differentiation required to specify cells as phloem (Bonke et al., 2003). *apl* mutants are seedling lethal and are typically devoid of phloem cell types at the phloem poles, namely sieve elements and companion cells. In a *fass* mutant background, APL was shown to regulate differentiation of the two phloem cell types as well as asymmetric division, and not simply proliferation since the *fass apl* mutant shows increased vascular cell numbers with xylem-like characteristics. Additionally, APL was shown to suppress xylem-associated tracheary elements when expressed throughout the vasculature, however it is not sufficient to cause ectopic differentiation into phloem.

Ground tissue (cortex and endodermis)

Asymmetric cell division is of particular importance for tissue fates in plants, due to the inherent lack of cell mobility. The cortex/endodermal initial cell, or CEI, generates two tissue types via sequential asymmetric divisions. After anticlinal division to regenerate the CEI and generate a daughter, the daughter cell divides periclinally. This second asymmetric division gives rise to the cortex and endodermis tissues, collectively referred to as the ground tissue (Figure 2). Subsequent cell fate specification depends on a unique mode of transcriptional regulation. *SHR* is transcribed in the stele, and upon translation, SHR protein moves to the surrounding endodermis, CEI, and QC, where it becomes nuclear localized and activates expression of target genes, including SCR (Bishopp et al., 2009; Helaruitta et al., 2000; Cui et al., 2007). SCR limits SHR movement by sequestration to the nucleus, where together they activate transcription of SCR and other patterning genes (Cui et al., 2007). *shr* mutants develop a single mutant layer of ground tissue which expresses markers for cortex tissue, suggesting a requirement of SHR in periclinal division of the CEI daughter cell and specification of endodermis (Helaruitta et al., 2000). *scr* mutants also exhibit a single layer of ground tissue, but with mixed endodermal and cortex identity (Di Laurenzio et al., 1996). After the second asymmetric division, SHR/SCR protein levels remain high in endodermal lineages, but drop precipitously in the cortex layer (Cui et al., 2007). Taken together, these results

support the hypothesis that endodermis tissue fate is dependent on SHR and SCR expression while the cortex fate is dependent on exclusion of these proteins.

Additional factors required for ground tissue patterning have been identified. MAGPIE (MGP), and its close relative JACKDAW (JKD), encode C2H2-zinc finger transcription factors which can interact with SHR and SCR in vitro (Welch et al., 2007). MGP is a direct target of SHR/SCR, and is expressed within the ground tissue and excluded from the QC. *jkd* mutants show ectopic periclinal divisions in the cortex resulting in increased numbers of cortex and endodermis cells. This phenotype is abolished in *jkd shr* mutants, suggesting that JKD acts through SHR to control ground tissue cell number. Additionally, SCR is down-regulated in the *jkd* mutant endodermis and induced in adjacent middle-cortex cells that originate from ectopic division of cortex suggesting that JKD may be required for proper SCR expression. Based on these data, Welch et al. proposed a model for QC and ground tissue specification in which SHR, SCR, and JKD influence QC identity; MGP, SHR, SCR, and JKD regulate CEI fate; and SHR and SCR promote endodermal cell fate (Welch et al., 2007). Interestingly, MGP and JKD expression is unaffected in double mutants for *PLETHORA1*/*PLETHORA2 (PLT1*/*PLT2)*, suggesting that PLT1/PLT2 transcription factors, known as 'master regulators' of root specification, act through an alternative mechanism for QC specification and stem cell activity (Welch et al., 2007).

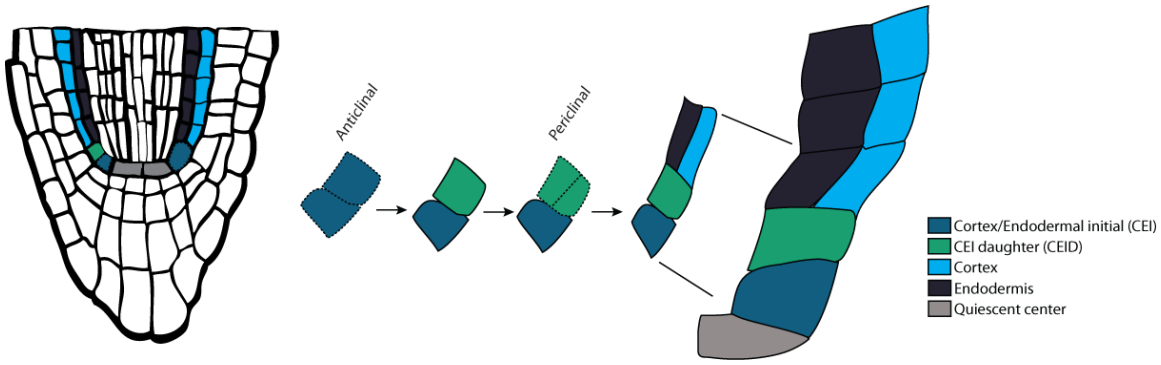

Figure 2: Schematic for ground tissue patterning. Anticlinal division of the cortex/endodermis initial cell produces the CEI daughter cell, which then divides periclinally to give rise to the endodermis (black) and cortex (purple) cell lineages.

Using an inducible system to drive SHR or SCR gene expression in a *shr* or *scr* mutant background, respectively, Sozzani et al. identified additional target genes controlling periclinal division of ground tissue (Sozzani et al., 2010). Periclinal cell division of the mutant tissue layer follows approximately six hours after either SHR or SCR induction, allowing genes modulated at the time of formative divisions to be identified. Based on GO category enrichment of transcription profiles following either SHR or SCR induction, the authors found an over-representation of cell-cycle progression and cyclin-dependent kinase (CDK) activity categories in both inducible systems. One of the genes identified, CYCD6;1, was found to be directly induced by SHR and SCR specifically in the CEI and its daughter cell at the time of asymmetric division (Figure 2). However, loss of CYCD6;1 function did not phenocopy shr mutants, suggesting roles for additional factors in regulating these formative divisions. By coupling pCYCD6;1::GFP reporter plants with fluorescence-activated-cell-sorting, the authors specifically isolated CEI/CEI-daughter cells for transcript profiling. Many

candidate genes emerged by pairing CEI-specific expression data with inducible SHR/SCR data. Two of these candidates, CDKB2;1 and CDKB2;2, as well as CYCD6;1 were then ectopically expressed in the ground tissue, with each exhibiting additional formative divisions in a wild type background. Additionally, partial complementation of ground tissue division in *shr* mutants was observed for CYCD6;1 and CDKB2;1 (Sozzani et al., 2010). Taken together, these data demonstrate a direct link between patterning regulation by SHR and SCR, and cell division, but also suggest that additional genes function to regulate formative divisions in the ground tissue.

Epidermis (non-hair and hair cells)

The epidermis is derived from initial cells that give rise to both epidermis and the lateral root cap (Dolan et al., 1993). The epidermis consists of two cell types, hair cells and non-hair cells, and their specification strictly depends on cell position (reviewed by Schellman et al., 2007 and Scheifelbien et al., 2009). Non-hair cells directly contact one underlying cortex cell, whereas hair cells lie over the junction between two cortex cells (Figure 3). A positional cue specific to the junction between cortical cells is thought to provide the hair cell fate signal, resulting in an alternating pattern around the circumference of the root. SCRAMBLED (SCM), which encodes a leucine-rich-repeat receptor-like kinase (LRR-RLK), is expressed throughout the developing root, and may transduce this hypothetical signal to the overlaying epidermal tissue (Kwak et al., 2008). In early developmental stages, SCM accumulates in both hair and non-hair cells in the

epidermis, but in the late-meristematic and early elongation zones, it localizes primarily to hair cells (Lee and Schiefelbein, 1999). Activated SCM represses transcription factor activity of the non-hair fate specifier WEREWOLF (WER; Kwak et al., 2005; Kwak et al., 2007; Yadav et al., 2008). In the non-hair cell, without positional activation of SCM repressor, WER, a MYB transcription factor, binds two bHLH transcription factors GLABRA3 (GL3) and ENHANCER OF GLABRA3 (EGL3; Lee and Schiefelbein, 1999). GL3/EGL3 also interacts with the WD40 domain transcription factor TRANSPARENT TESTA GLABRA1 (TTG; Payne et al., 2000; Zhang et al., 2003). Together, these form a large complex (the WER complex) that promotes transcription of GLABRA2 (GL2), a homeodomain transcription factor required for non-hair cell fate specification (Bernhardt et al., 2003; Lee et al., 2002). CAPRICE (CPC), another Myb transcription factor, is also activated by this complex in non-hair cells and moves to neighboring hair cells where it acts with the MYB factors TRIPTYCHON (TRY) and ENHANCER of TRY to promote hair cell fate (Lee et al., 2002; Ryu et al., 2005; Koshino-Kimura et al., 2005; Kurata T, 2005; Kirik et al., 2004; Schellmann et al., 2002; Simon et al., 2007). Most epidermal cells of *wer* knockout mutant roots take on the hair cell fate, whereas *cpc* mutant roots have very few hairs compared with wild type (Kwak and Schiefelbein, 2008; Wada et al., 1997). Downstream epidermal patterning events are less clear, but appear to involve phosopholipid signalling mediated by GL2 (Ohashi et al., 2003).

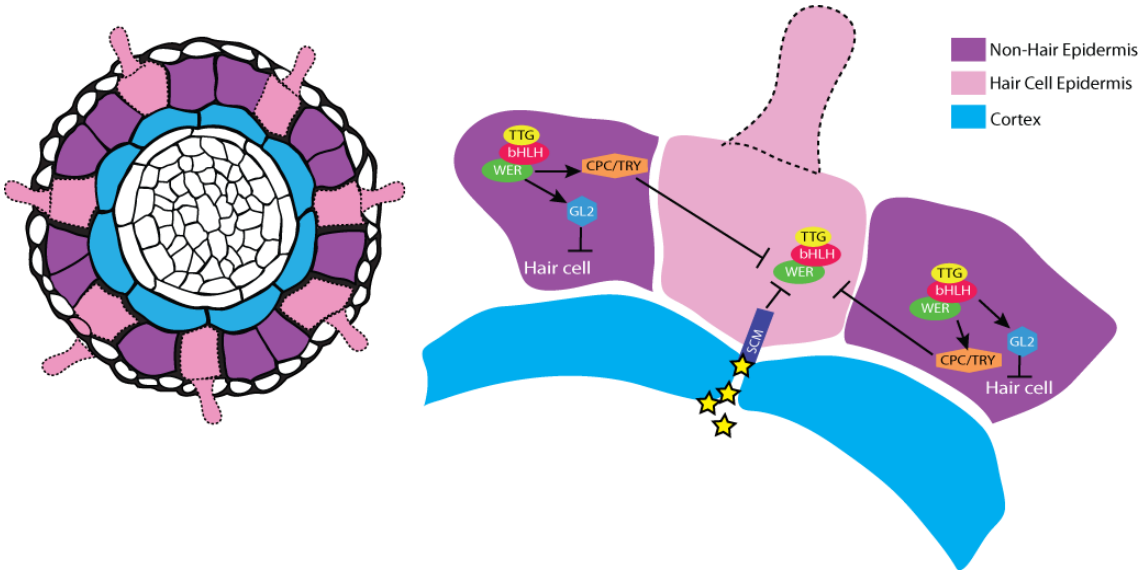

Figure 3: Model for epidermal patterning. An unknown signal (yellow stars) activates the *SCRAMBLED* (SCM) receptor-like kinase localized to the epidermal cell membrane which lies between a cortex-cortex cell junction. Activated SCM represses the "hair cell" repressor *WEREWOLF* (WER), thus allowing for specification of the hair cell fate.

Hormonal control in development

Phytohormones act as key intercellular signals throughout plant development. Although nearly all of the major phytohormones play some role in post-embryonic primary root development, we focus here on auxin, cytokinin, and gibberellin.

Auxin is a key phytohormone that has been implicated in nearly every developmental process. Auxin is transported between plant cells by several different families of transporters. Root development hinges on the polar auxin transport mediated by the eight-member PIN polar auxin transporter family. The PINs have different distributions in different cell types, and their distribution directs an auxin reflux loop in the root that is important for stem cell niche maintenance (Feraru and

Friml, 2008; Blilou et al., 2005; Grieneisen et al., 2007). Basal distribution of specific PINs in the stele directs auxin flow rootward, reaching a maximum level in the root tip in the stem cell niche (Blilou et al., 2005; Friml et al., 2004). Auxin is then laterally redistributed in the columella, and then transported shootward in the epidermis and lateral root cap (Feraru and Friml, 2008; Blilou et al., 2005; Friml et al., 2002; Muller et al., 1998). It then re-enters the vasculature in the transition zone and flows back toward the stem cell niche, thereby maintaining the maximal level in the root tip. The maximal point at the root tip is stable, but is dynamic in the transition zone, allowing for growth and differentiation as described below. The gradient of PLT expression in the root meristem suggests that these genes can act as transcriptional 'outputs' for auxin (Grieneisen et al., Galinha et al., 2007). *PLT* genes, in turn, control the expression of *PIN*s creating a robust regulatory circuit (Smith et al., 2010; Galinha et al., 2007).

A second, parallel pathway involving the GRAS family transcription factors SCARECROW (SCR) and SHORTROOT (SHR) is also important for stem cell niche maintenance. As previously described, *SHR* is expressed in the stele and moves one cell layer into the endodermis and QC, where it activates transcription of *SCR* (Nakajima et al., 2001). The overlap between the highest level of *PLT1* and *PLT2* expression and the SHR and SCR transcription factor protein domains defines the stem cell niche (Scheres B, 2007).

In addition to their roles in stem cell maintenance, phytohormones play a role in controlling meristem size. For example, in the root meristem, auxin promotes cell division, while cytokinin promotes cell differentiation. In order to maintain continuous growth, the root must balance the rate of cell division in the meristematic zone with the rate of cells leaving the zone to differentiate. Recent work has shown that interactions among auxin, cytokinin, and gibberellin, are crucial for determining and maintaining meristem size (Dello Ioio et al., 2007; Dello Ioio et al., 2008; Moubayidin et al., 2010; Ruzicka et al., 2009; Ubeda-Tomas et al., 2008; Ubeda-Tomas et al., 2009).

Meristem size actively increases from germination to approximately 5 days post germination (DPG), when a balance is achieved between cell division and differentiation, and final meristem size is set. Meristem size is maintained through the antagonistic action of cytokinin and auxin (Dello Ioio et al., 2007; Dello Ioio et al., 2008; Moubayidin et al., 2010; Ruzicka et al., 2009). Cytokinin controls the expression of the cytokinin response regulator *ARR1*, which activates the auxin AUX/IAA repressor *SHY2*. SHY2 represses expression of the *PIN* polar auxin transporters, restricting rootward and lateral distribution of auxin, and promoting cellular differentiation. Conversely auxin causes the degradation of SHY2, relieving *PIN* gene repression and allowing auxin flow throughout the root, promoting cell division. Thus the antagonistic interaction between cytokinin and auxin results in a balance between cell division and cell differentiation.

Although this model nicely describes the maintenance of meristem size, it does not provide answers for how the final size is set. During meristem growth, cell division must outweigh differentiation. In line with this, further work showed that *ARR1* expression is low prior to 5 DPG, and that *SHY2* is not strongly activated until this point. In addition to its activation of *ARR1*, cytokinin also controls the expression of *ARR12*, which promotes a low level of *SHY2* expression prior to 5 DPG. At 5 DPG, both ARR1 and ARR12 are present, increasing the level of *SHY2* expression, thus reducing *PIN* expression and auxin flow. This results in increased cell differentiation, which balances with ongoing cell division and sets meristem size (Moubayidin et al., 2010). In further support for this model, *PIN* gene expression is higher at 3 DPG and decreases at 5 DPG (Moubayidin et al., 2010).

This work also showed that *ARR1* expression is kept low until 5 dpg by the action of another hormone, gibberellin (GA; Moubayidin et al., 2010). Exogenous GA increases meristem size at 5 DPG, but has no effect when applied earlier. *arr1* mutants are insensitive to GA at 5 DPG, and *ARR1*:GUS expression is downregulated after exogeneous GA application, suggesting that GA mediates root meristem size through ARR1 (Moubayidin et al., 2010). This leads to a model where, prior to 5 DPG, gibberellins repress cytokinin signaling through ARR1. This keeps levels of SHY2 protein low, as only ARR12 is present to activate *SHY2* expression, allowing *PIN* gene expression and promoting auxin flow and cell division. At 5 DPG, levels of gibberellins

decrease and cytokinin signaling through *ARR1* is activated. This leads to high levels of SHY2 protein, repressing *PIN* expression and promoting cellular differentiation, thereby balancing cell division and differentiation, and setting final meristem size (Moubayidin et al., 2010).

In addition to their role in the pathway described above, gibberellins also play a role in the control of meristem size and root growth through specific interactions in the endodermis. Expression of a non-degradable form of the DELLA protein GA Insensitive (GAI) specifically in the endodermis resulted in decreased root growth (Ubeda-Tomas et al., 2008). Endodermal cells of roots expressing the mutant form of GAI in the endodermis failed to fully expand. Furthermore, epidermal and cortex cells of these lines expanded radially, causing severe bulging in the epidermis. This expansion of the outer cell types did not occur when the mutant form of *GAI* was expressed throughout all tissues in the root, although cells in the meristem were all shorter. Thus GA signaling throughout the root is necessary for normal root growth and development, but signaling in the endodermis is important for anisotropic growth in the surrounding cell types and tissues, possibly to coordinate expansion among all the tissues (Ubeda-Tomas et al., 2008).

Finally, in addition to regulating cell expansion in the root, GA is also thought to control cell division (Ubeda-Tomas et al., 2009; Achard et al., 2009). Similar to auxin-deficient mutants, GA-deficient mutants have smaller meristems (Ubeda-Tomas et al.,

2009; Achard et al., 2009). GA appears to regulate meristem size in the root by regulating mitotic activity, as the GA-deficient mutant *ga1-3* has reduced cell numbers in the meristem, and the number of dividing cells is reduced compared to wild type (Ubeda-Tomas et al., 2009; Achard et al., 2009). The decrease in cell division is not simply the result of decreased stem cell niche identity, as treatment with either GA or a GA inhibitor resulted in no change in expression or localization of stem cell markers in the root (Achard et al., 2009). Thus GA appears to regulate root growth both in terms of cell size and cell proliferation.

In addition to cytokinin, auxin and gibberellins, the hormones brassinosteriods (BRs), ethylene, and abscisic acid (ABA) also play roles in controlling meristem size and root growth. Recent work has demonstrated that the small meristem size of BR-signaling deficient mutants is due to both impaired cell cycle activity and reduced cell expansion (Ubeda-Tomas et al., 2009; Achard et al., 2009). Further, BR-activity in the epidermis is sufficient to control meristem size (Ubeda-Tomas et al., 2009). Ethylene inhibits root growth, particularly root cell elongation, in part through cross-talk with auxin and cytokinin (Stepanova et al., 2007; Swarup et al., 2007; Ruzicka et al., 2009). Ethylene has also been shown to have a role in the production of stem cells in the root meristem (Ortega-Martinez et al., 2007). Mutations in the E3 ligase *ETHYLENE OVERPRODUCER1 (ETO1)* lead to divisions in the QC. The *eto1* mutant produces excessive amounts of ethylene. When *eto1* mutants were grown in media supplemented

with an ethylene biosynthesis inhibitor, no extra divisions were observed in the QC. Further, growing wild type plants in the presence of ethylene induced divisions in the QC. The extra cells behaved like QC cells in that they were able to repress the differentiation of surrounding stem cells and expressed QC-specific genes. Together these results suggest that ethylene promotes cell division in this cell type (Ortega-Martinez et al., 2007).

In contrast to ethylene, blocking ABA biosynthesis in seedlings induces division in QC cells (Zhang et al., 2010). The effect is dose-dependent, and occurs in as many as 50% of the roots exposed to an ABA inhibitor. QC divisions (at various frequencies) are also found in ABA-biosynthesis mutants. Further, roots treated with an ABA biosynthesis inhibitor show terminal differentiation of the QC and columella stem cells. The results suggest that ABA promotes QC quiescence and suppresses stem cell differentiation in the root. This work also has implications for root growth and development in stressful environments. Root growth is often inhibited under abiotic and biotic stress, but can resume once the stress is removed. Since ABA plays a role in many stress responses, this work may explain how roots growing in stressful conditions maintain their stem cell populations so they can continue to grow when the stress is removed.

1.2 Stress and development

Plants are immobile, so dealing with harsh conditions is inevitable. Therefore, plants have evolved to adapt growth programs to deal with stresses from the environment. Interactions between growth and stress responses are not clear, but this work and that of others begins to identify genes acting at this interface. Recent studies from our lab compared transcriptomic data from plants stressed in four ways: exposure to high salt-, acidic-, low iron-, and low sulfur-conditions, and found that many stress responses were tissue-type-dependent (Dinneny et al., 2008; Iyer-Pascuzzi et al., 2011). Interestingly, Iyer-Pascuzzi found that mutants for many key developmental regulators exhibited hypersensitivity to the stress-responsive hormone ABA, and the transcription factor *SCARECROW* (*SCR*) directly binds to promoters for known stress-responsive genes, providing direct evidence linking stress response to development.

1.3 Phosphate deprivation

Inorganic phosphate (P_i) is an essential nutrient required for many metabolic processes, but is highly reactive with soil constituents rendering it mostly unavailable for uptake. Therefore, plants have evolved strategies to survive periods of deprivation, or limited availability, as well as to increase nutrient acquisition potential. Physiologically, roots exude phosphatases to solubilize organic forms of P_i making it available for uptake and high-affinity transporter proteins are induced to increase absorption and transport throughout the plant (Okumura et al., 1998; Hinsinger et al.,

2001; Misson et al., 2004; Smith et al., 2011; Remy et al. 2012). Following depletion of local soluble resources, root systems change structurally by increasing absorptive surface area through emergence of root hairs and extending lateral roots to "explore" soil matrices for additional P_i (Ma et al., 2001; Lopez-Bucio et al., 2002). Therefore root morphology is important for acquisition of this nutrient, making response to P_i– deprivation a model for studying regulation of root developmental modulation or morphogenesis. Additionally, elucidation of mechanisms controlling root development in response to low Pi-availability carries implications for crop security. Due, in part, to dwindling Pi resources, agricultural demands have pushed Pi-rich fertilizer costs up dramatically in the last several years (National Agricultural Research Service, USDA report 2012). A clearer understanding of how root development is modulated in response to deprivation may provide insight into strategies for efficient Pi use.

Due to the fiscal and environmental costs associated with Pi-fertilizer use, several groups have studied aspects of response. Although details are unclear, a few mechanisms have been proposed. It is currently thought that Pi is solubilized by secreted acid phosphatases and taken in at the root-soil interface by high- and low-affinity transporters (Miller et al., 2001; Wang et al., 2011). This cannot exclude the possibility of passive passage into the freely diffusible space between cells, termed the apoplast. Either way, once Pi reaches the vasculature, it is loaded into the root xylem by PHO1, an SPX-domain containing transporter, for transport throughout the plant

(Hamburger et al., 2002). Meanwhile, microRNA (miR) 399 targets the transcript encoding an E2 ubiquitin ligase, *PHO2*, for destruction (Chiou et al., 2006). Repression of PHO2 relieves repression of Pi-responsive genes, like *PHO1* and others, allowing plants to accumulate higher levels of Pi particularly in the shoot (Liu et al., 2012). Roles for transcription factors of several families, SUMO-ligase, and a vesicular trafficking protein have also been demonstrated, but with little understanding of location of activity (Miura et al., 2005; Bari et al., 2006; Bustos et al., 2010; Bayle et al., 2011).

Many groups have carried out transcriptomic analyses to identify Pi-responsive genes (Hammond et al., 2003; Wu et al., 2003; Misson et al., 2005; Muller et al., 2007). Currently, it is thought that early in response, plants initiate a general stress response followed later by events specific to Pi-deprivation. This could be due to buffering within plants that allow for growth during periods of deprivation. Unfortunately, little agreement exists between these studies demonstrating that transcriptomic responses vary widely depending on growth conditions (e.g. hydroponics versus solid media), plant age at transfer, low Pi-exposure timing, and lighting conditions (i.e. due to carbon fixation). Types of tissues profiled will affect interpretation of data as well. In fact, the tissues assayed included whole plant or whole root and leaf tissues for expression analysis, leaving open questions about responses within individual tissues. All of these factors have led to a poor understanding of underlying responses to Pi-deprivation, leaving many open mechanistic questions.

In order to reconcile what is known about response to Pi deprivation, it seems necessary to understand how individual tissues or regions within roots respond. Svistoonoff et al. demonstrated that root tips are involved in sensing Pi and subsequent architectural reprogramming to increase acquisition potential (Svistoonoff et al., 2007). The authors proposed that a decrease in primary root length depends on meristem exhaustion which follows sensing of Pi levels through the multi-copper oxidase (*LPR1*). Additionally, Ticconi et al. showed that the ATP-ase *PHOSPHATE DEFICIENCY RESPONSE 2*co-localizes in the endoplasmic reticulum with *LPR1* and is required for the patterning regulator *SCR* (Ticconi et al., 2009)

1.4 Statement of problem and hypothesis

To begin linking genes directly to aspects of developmental modulation in response to Pi-deprivation, we aimed to describe phenotypic changes to roots with high resolution, to conduct systematic expression studies with tightly controlled exposure times and growth conditions, and to exploit tools used to isolate specific root tissues. Our hypothesis is that early transcriptional modulation leads to changes in root morphology and that identification of genes controlling small changes will provide insight into how developmental programs are modulated to affect the entire root.

Chapter 2. Screen for changes to cellular morphology in response to phosphate deprivation

In an effort to increase the spatial resolution at which root responses were described, we used confocal microscopy to visualize root tips over a time-course of exposure to low phosphate. With an understanding of response at the level of tissue organization and cell morphology, we aimed to bring our tools for expression analysis closer to the mechanisms underlying root responses to Pi-deprivation. After screening many GFP-expressing reporter lines, we made novel observations that added to our understanding of how the root developmental program is modulated under these conditions.

2.1 Methods

Plant growth conditions

All adult plants were grown on a 16-hour day/8-hour night schedule in a temperature and humidity controlled growth chamber at 22°C. Plants were watered and fertilized as needed, and were treated with Gnatrol insecticide, once.

For all experiments, seeds were surface sterilized using one of the following methods: (1) 10 minute agitation in 50% bleach, 0.1% Triton-X100 followed by 1 minute in 70% ethanol, or (2) 1-3 hours in an air-tight chamber with a reaction mixture of 60ml bleach and 2ml 12M HCl. Seeds were allowed to imbibe in the dark for 1-3 nights at 4°C. After sterile plating on 1X MS, 1% sucrose, 1% agar media (control plates; Caisson

catalog #MSP01, BD Difco catalog #214510) and sealing with parafilm or porous tape, seedlings grew vertically on square agar plates in a growth chamber with 16-hour days/8-hour nights unless otherwise specified.

Tissue-specific time-course expression microarrays

GFP reporter line seeds were surface sterilized with 50% bleach, 10% Triton-X100 for 10 minutes and 70%ethanol for 1 minute. Seeds were plated on control media with mesh in two rows with a depth of 1 seed and a total of 60-80 seeds per plate, and sealed with porous tape. Seedlings were grown under 16h days/8h nights or continuous light. Seedlings were transferred to control or 1XMS without phosphate, 1% sucrose, 1% agar media (low Pi; Caisson catalog #MSP11) at 4days post imbibition, and exposed for 24 (control and low Pi), 36 (low Pi), and 48 (low Pi) hours prior to tissue collection. Cells of root tips were enriched for by cutting approximately 1-2 millimeters from the root tip, followed by enzymatic digestion and FAC-sorting to yield GFP-marker protoplasts for lines marking the cortex cell lineage (*pCO2:YFP*), endodermis lineage (*pSCR:GFP*), and epidermis lineage (*pWER:GFP*).

Confocal microscopy and RootArray

Using an upright confocal microscope, live roots were imaged for medial and longitudinal optical sections of the root apical meristem in a plane positioned 5 cortex cells above the quiescent center (white line in picture at left). Cells were counted around the root circumference for several tissue types. For circumference size, the length of the

smallest perfect circle around the cortex tissue layer was measured (red circle) using LSM software.

For direct germination, sterile seeds were placed directly on P_i-sufficient/control (1XMS, 1%sucrose) or P_i-deficient (1X MS without Pi, 1% sucrose) media and imaged at 5 days post imbibition. For transfer experiments, seeds were placed on P_i-sufficient media for 3days and seedlings were moved to either control or P_i-deficient plates.

The RootArray platform was used for whole meristem, 3-D imaging. pCO2:YFP-H2A/Col-0 seeds were soaked for 2-3 nights in water at 4°C, and sown and sterilized within a micro-fluidic growth chamber called a RootArray (Busch et al., 2012; Heidstra et al., 2004). Grown under continuous light at room temperature, seedlings grew for 5days in liquid 1XMS, 1% sucrose media before switching to 1XMS without Pi, 1% sucrose. Roots were imaged over time at an interval of 1-1.5 hours.

2.2 Results and discussion

Developmental modulation in response to Pi-deprivation

To observe significant changes in root length and growth rate, we performed transfer experiments. We found that significant changes to primary root growth rate were observed after three days of exposure to low P_i (Figure 4A). Slowing in growth rate continued after four and five days, ultimately leading to growth arrest. Additionally, emerged root hair density increased near the root tip by three days of exposure (Figure 4B). We hypothesized that underlying regulation of structural changes

with respect to primary root elongation and root hair emergence occurs prior to this point in time. Therefore, we focused our studies prior to three days of exposure to elucidate early events in plant responses to P_i-deprivation.

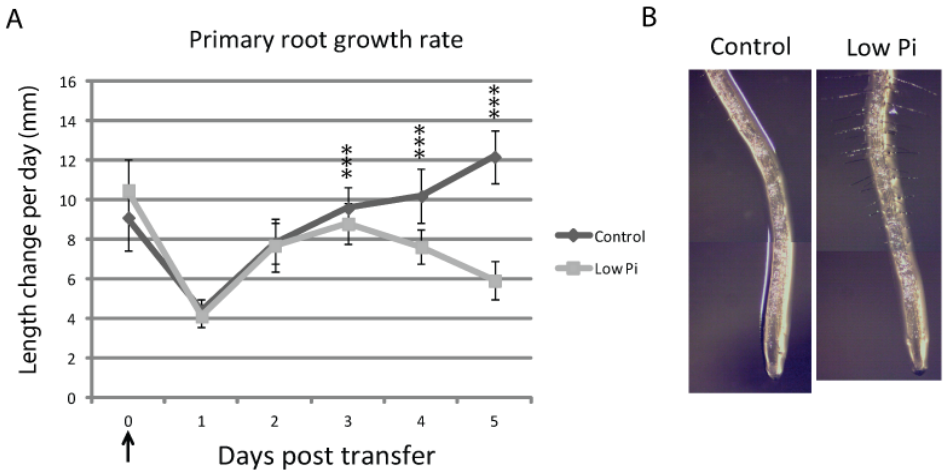

Figure 4: Root developmental modulation in response to Pi deprivation. (A) Primary root growth rate slows significantly by three days of low Pi exposure, eventually halting. Length of 5DPI roots at point of transfer marked by arrow. (C) Images of Col-0 roots show an increase in emerged root hair density three days after transfer to low Pi media. ***p<0.001

In an effort to visualize the changes in morphology at cell-type resolution, we observed wild type plants expressing GFP under the control of several tissue-specific promoters. We focused on tissues of the stem cell niche and root meristem. We observed meristem disorganization in vascular reporter lines, but no change to reporter expression domain for markers of the phloem, phloem-pole pericycle, and xylem (Appendix A, Figure 15). To understand causes of meristem disorganization, we screened for changes to reporter expression or cell morphology within tissues surrounding the vascular cylinder, namely cells of the QC, pericycle, endodermis and

cortex tissues. The observed disorganization of the meristem showed increasing severity over time with the QC hardly recognizable beyond four days on low P_i (Figure 9A). Interestingly, we observed expansion of reporter expression for markers of the QC suggesting that low P_i-induced disorganization could be due, at least partly, to divisions of the QC or ectopic expression of QC-specific genes in the surrounding stem cells and adjacent tissues. QC divisions leading to differentiation of root stem cells could support a model for exhaustion of the root apical meristem, which provides a possible mechanism to halt primary root growth. The events upstream of these divisions are unclear, but do appear to involve redistribution of the hormone auxin which is transported apically and accumulates to high levels in the QC to control expression of many developmental genes (Figure 9B; Benkova et al., 2003).

Upon further inspection, we observed an increase in the number of endodermis and cortex cells in a transverse plane near the QC (Figure 10A and C), and that this increase leads to an increase in meristem circumference (Figure 10D). In order to determine where additional cortex cells were made, we used the RootArray (Busch et al., 2012) platform to visualize growing roots in 3D. The *pCO2:YFP* marker revealed that contiguous "strings" of recently divided cortex cells exist near the QC as well as higher in the meristematic zone (Figure 10B; Heidstra et al., 2004). Reconstruction of RootArray images enabled us to see that these strings of divisions are not physically connected suggesting that stem cell divisions are not wholly responsible for the increase in

circumferential cortex cell number, but rather that cortex cells may divide in the periclinal plane following specification. The cortex divisions described here phenocopy mutants for the patterning regulator *JACKDAW,* the katanin protein *ECTOPIC ROOT HAIR3,* and the vacuolar sorting protein *SHRUBBY (JKD, ERH3, SHBY;* Webb et al., 2002; Hassan et al., 2010; Koizumi et al., 2013*).* We hypothesize that these proteins influence this aspect of developmental modulation in response to low Pi.

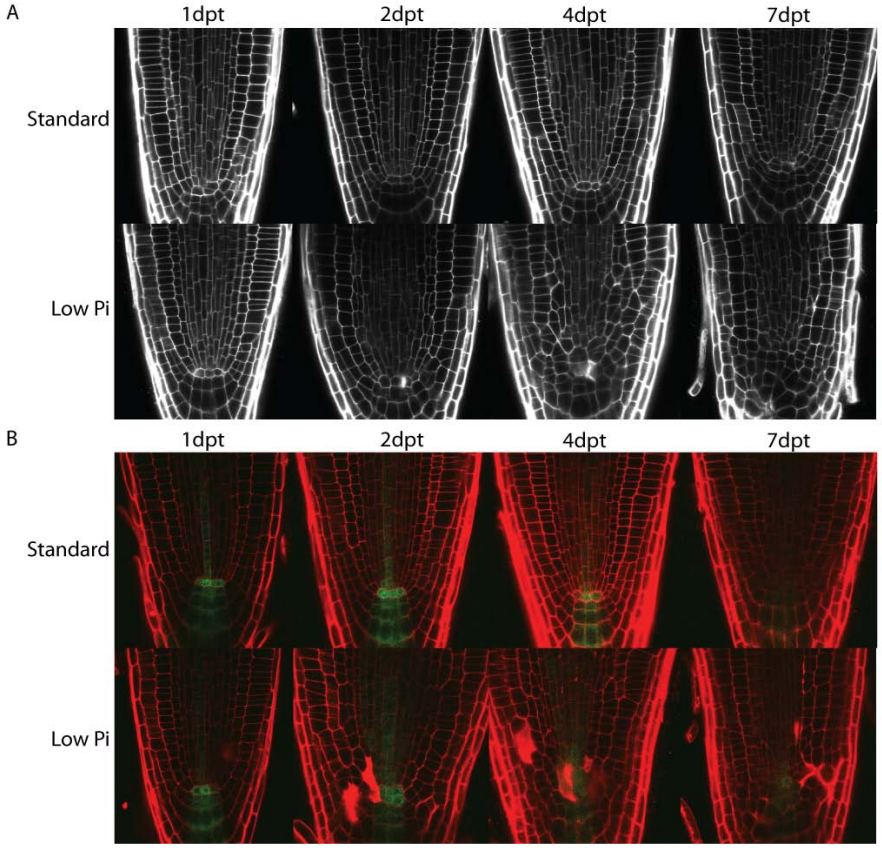

Figure 5: The stem cell niche and meristem become disorganized in response to Pi deprivation. (A) Medial longitudinal sections of root stem cell niche and meristem show disorganization by 2 days post transfer (DPT) with increased severity over time. (B) pDR5:GFP marker shows expansion of the auxin-marked quiescent center cells.

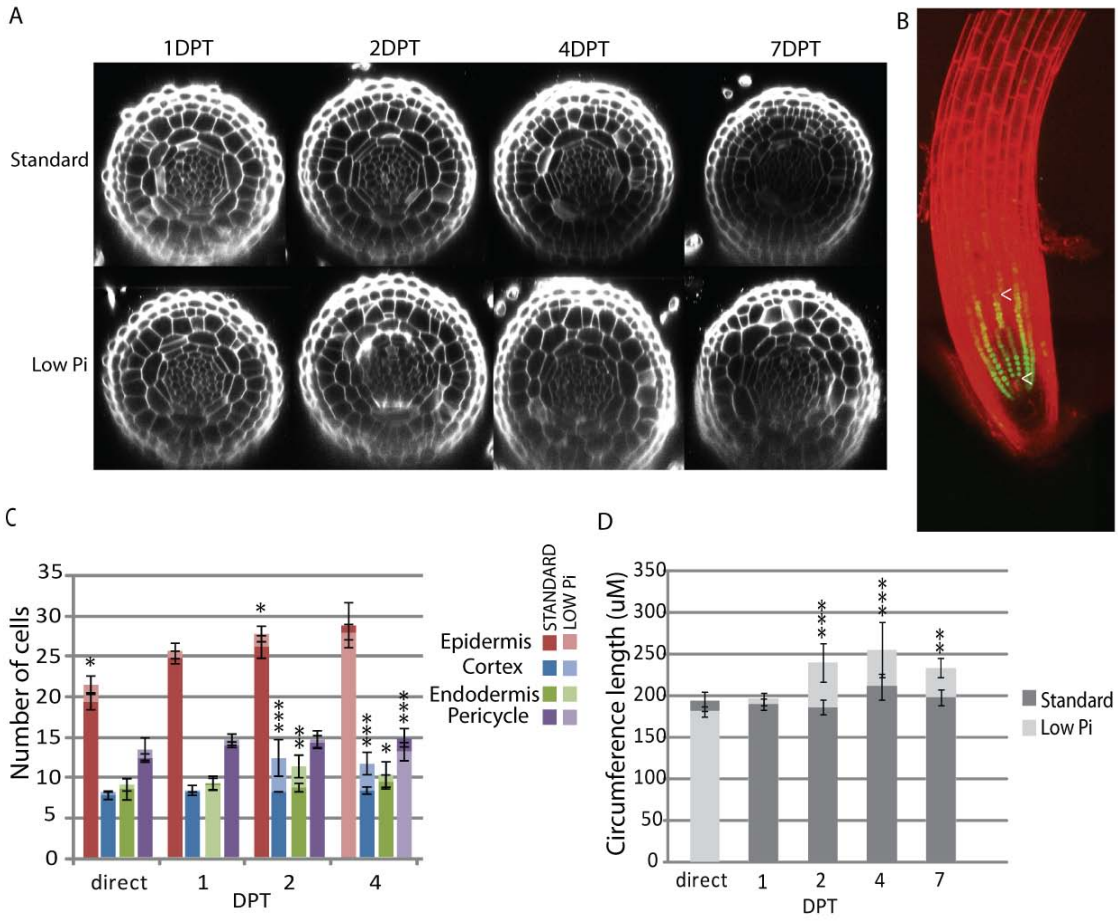

Figure 6: Root cell divisions mark early response to Pi-deprivation. (A) Transverse optical sections show an increase in number of circumferential cortex cells after two days post transfer to low Pi (DPT) and continuing through time-course. (B) 3D reconstructed image of pCO2:GFP-H2A reporter marking cortex nuclei after approximately 40 hours in Pi-free media. White arrowheads mark bifurcation point of cortex nuclei. (C) Chart of circumferential cell number for epidermis (red), cortex (blue), endodermis (green), and pericycle (purple). Significant increases observed on low Pi for cortex and endodermis by two DPT and significant decrease in pericycle number by four DPT. (D) Circumference length around cortex and internal tissues show significant increases by two DPT. ***p<0.001, **p<0.01, *p<0.05

We hypothesized that developmental modulation resulting in additional cortex-cortex cell junctions provides a means for additional specification of epidermal root hairs, possibly via activation of the *SCRAMBLED* pathway (Kwak and Schiefelbein,

2007). We found that deprivation of P_i results in an increase in the number of epidermal cells specified as hair cells around the root circumference (Figure 11). Occasionally, we also observed hairs emerging from directly over a single cortex cell, which had been suggested as the mechanism to achieve extra hairy roots in response to low Pi (Appendix A, Figure 16; Muller and Schmidt, 2004). These results support a novel, although not exclusive, model for low Pi-induced root hair specification. Following cortex divisions that occur in response to low Pi, additional root hairs are specified through the canonical process (Kwak and Schiefelbein, 2007).

Robustness of developmental programs is hard to test, particularly in a developmentally plastic organ such as the root. We wondered, though, if response to low Pi varied depending on seedling age at transfer. We found that seedlings transferred at 3DPI showed significant, albeit smaller, increases in circumference length and epidermis, cortex, and endodermis cell number after 4 days on low Pi (Appendix A, Figure 17). This contrasts with our finding that timing of significant cell number increases in response to low Pi occurs after just two days when seedlings are 5DPI in age upon transfer. Interestingly, the true age of plants at the time of response (7DPI) is similar, suggesting that 3DPI seedlings are too young to respond with respect to circumferential morphology. I hypothesize that hormones play a part in the root's ability to respond by altering circumferential length and cell number because changes in levels of GA (decrease) and cytokinin (increase) occur around 5DPT (Moubayidin et al.,

2010). Additionally, Martin et al. showed that although expression of several Pi-responsive genes is inhibited by cytokinin application, root hair density is not repressed (Martin et al., 2000). Taken together, these data suggest that cytokinin hormone may be required for Pi-responsive root hair density increases. And we hypothesize that the cortex divisions described here depend on cytokinin levels.

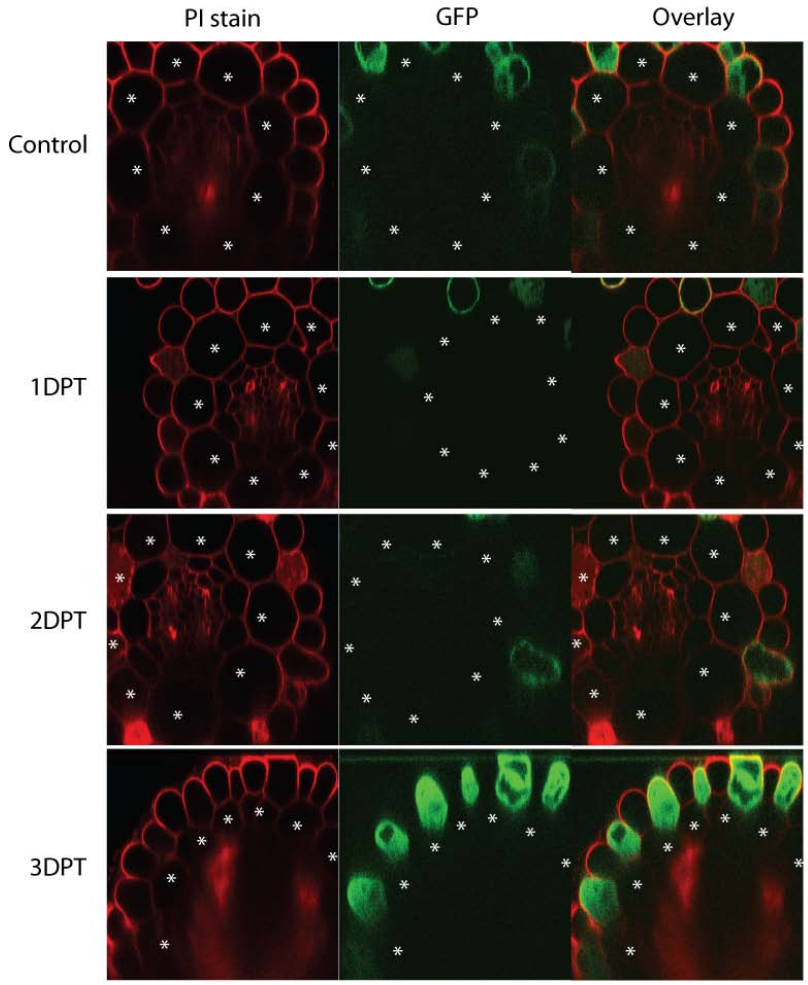

Figure 7: Root hair specification under low Pi conditions. At 3 DPT, roots appear to have more root hairs than controls (Figure 4B). Transverse optical sections reveal that by 3DPT, additional epidermal cells express the root hair marker *pCOBL9:GFP* (4th panel). White stars mark cortex cells.

Tissue-specific expression analysis

In an effort to identify genes controlling the increase in circumferential cortex and endodermis cell numbers, we profiled meristematic cortex and epidermis cells isolated by FAC-sorting following exposure to low P_i. We determined the exposure-time necessary to enrich for dividing and divided cells using confocal microscopy, so that expression analysis would capture time-points before and after divisions in addition to controls. Many genes upregulated by Pi-starvation show induction by 2-fold or greater over control in cortex and epidermis tissues, including several phosphatases and phosphate transporters, as well as the phosphate transport facilitator *PHF1*, the phosphate starvation-induced permease *ATPS3*, the sulfolipid biosynthesis enzyme *SQD1*, and the SPX-domain protein *SPX1* (Appendix A, Tables 1 and 2; Patel et al., 1998; Li et al., 2002; Gonzalez et al., 2005; Miura et al., 2005; Hammond et al., 2003; Wang et al., 2004). Interestingly, expression of a short peptide called *ROOT MERISTEM GROWTH FACTOR3 (RGF3)*, showed 2-fold induction after 24 hours in cortex tissue and after 36 hours in root epidermis (one of only six genes induced in both tissues). *RGF3* was previously shown to influence meristem size, with respect to length (Matsuzaki et al., 2010), making this gene a candidate regulator of the anti-clinal divisions described here.

2.4 Future directions

Based on induction of *RGF3* specifically within cortex and epidermis tissues close to the time of circumferential division response, I hypothesized that the short peptide

protein regulated these divisions. RGF3 is thought to act redundantly with RGF1 and RGF2 to modulate size of the transit amplifying cell population within the root meristem. Since we observe divisions of cortex cells in the transverse plane, we will use *rgf1rgf2rgf3* triple and single mutants to ask whether cortex divisions take place in response to low Pi when these genes are knocked-out. My prediction is that one or all of these gene products play roles in modulating anti-clinal division of meristem tissues in response to low Pi. If preliminary results replicate, RGF2 is required for cortex divisions by 2DPT on low Pi. I will repeat this experiment with a time-course of four days to understand whether knocking out RGFs lead to delayed response or no response at all. This will be the first demonstration of a signaling peptide acting to modulate morphology in response to environmental perturbation. It will be interesting to see if *rgf2* mutants do not increase the density of specified root hairs on low Pi, which is my prediction because these mutants do not exhibit cortex divisions as a response. Also, I treat *rgf2* mutants with RGF1 peptide after low Pi exposure to elucidate redundancy between these peptides. This work begins to build links between low Pi response, tissue-specific expression modulation, anti-clinal cortex and epidermis divisions, and root hair specification, supporting a model that will continue to be studied and expanded. In collaboration with others in the lab, we also aim to identify transcription factors that regulate expression of RGF2 using yeast-1-hybrid. This will allow us to add to our model by building a transcriptional network underlying these divisions.

To complement the expression study, we will conduct a forward genetics screen to identify additional mutants that do not respond to low Pi by dividing in the cortex cell layer. An EMS-mutagenized population was generated in the lab, and we aim to exploit the high-throughput capacity of the RootArray imaging platform to screen these mutants for lines that do not respond to a switch from complete to Pi-depleted media.

Chapter 3. High resolution expression profiling reveals tissue-specific regulator of low-phosphate dependent root morphogenesis

Root developmental programs constantly integrate information from the environment, such that availability of nutrients within the soil space can lead to modulation of root morphology. Due to the fiscal and environmental costs associated with deprivation of the essential macronutrient Pi, several groups have identified and studied Pi-responsive genes. These works have focused on changes beyond 6 hours of exposure, leaving the earliest time-points unexplored. Additionally, many groups have performed expression analyses to identify nodes in a "Pi-response" network using methods with low spatial resolution (e.g. whole root, shoot, and plant tissues). Here, we describe the early transcriptional and morphological events occurring in response to Pi deprivation as more recent work suggests that individual tissue domains (or cell types) within roots express unique transcriptional profiles not only during development, but in response to abiotic stress (Brady et al., 2007; Dinneny et al., 2008; Iyer-Pascuzzi et al., 2010). By querying individual root tissue- and developmental-domains for transcript modulation in response to Pi-deprivation, we characterized transcript expression modulation with high spatial resolution and identified putative regulators of the early events of morphogenesis.

When deprived of P_i, an essential yet immobile nutrient, plants respond by reducing primary root elongation/growth rate and increase root hair outgrowth. To

examine these developmental shifts with high resolution, we performed a reverse genetics screen based on expression modulation within specific tissue domains.

3.1 Methods

Whole root time-course expression microarray

Columbia-0 (Col-0), or wild type, seeds were surface sterilized and plated with water at a density of 12-14 seeds per plate on mesh sheets overlaid on standard plates and sealed in Parafilm. Seedlings, age 5 days post imbibition (DPI) on mesh were transferred to low Pi media for a period of 0 (transferred and roots collected immediately; control), 1, 3, 6, 12, 24, or 48 hours. Whole root tissue was collected and pooled at noon for each time-point analyzed, and was snap-frozen in liquid nitrogen. Two biological replicates were prepared for each time-point. Total RNA was isolated according to manufacturer's instructions (Qiagen RNeasy Mini Kit catalog #74104). RNA was precipitated overnight with ammonium acetate at -20°C in the presence of Glycoblue reagent. Using the Affymetrix One-Step Amplification kit (Catalog #900431), mRNA was amplified, labeled, and fragmented. Hybridization to Affymetrix ATH1 Expression Microarray chip was carried out according to manufacturer's instructions by Expression Analysis Inc.

Developmental zone microarray

Columbia-0 seeds were surface sterilized and plated as described above. At exactly 5 DPI, seedlings on mesh were transferred to standard or low Pi plates. Tissue

was collected between 8:00 and 9:30am after 3 hours of exposure to low Pi. For tissue collections, seedlings were hand-dissected into four developmental zones as described (Dinneny et al., 2008). All tissue sections originated from the same 40 roots. Two biological replicates were prepared for each sample. Total RNA was isolated and precipitated as described above, except that Qiagen RNeasy Micro kit was used. Using the Affymetrix 3' IVT Amplification kit (Catalog #901228), mRNA was amplified, labeled, and fragmented. Hybridization to Affymetrix ATH1 Expression Microarray chips were carried out according to manufacturer's recommendations by the Duke University Microarray Core Facility.

Cell- or tissue-specific expression microarray

Seeds of GFP-expressing reporter lines (i.e. GFP expressed under control of promoters for the following genes or regions in the Columbia-0 background: PET111, SCR, WER, COR315.1, COBL9 and WOL) were surface sterilized and plated as described above, except that the density of seeds per plate was increased to two rows of approximately 50 seeds. At exactly 5 DPI, seedlings on mesh were transferred to standard or low P_i plates. Roots were harvested after 3 hours of exposure between 8:00 and 9:30am (i.e. root tips only for PET111, but whole roots for all other lines), and cut into small pieces. Cell walls were enzymatically digested to release intact protoplasts and GFP-marked cells were enriched using fluorescence-activated-cell-sorting (FACS; Birnbaum et al., 2005). Three biological replicates were prepared for each sample. Total

RNA was isolated and precipitated, and microarray expression analysis was performed as described for developmental zones.

Expression data analysis

Mean expression values were determined for each perfect-match probe-set and mixed-model ANOVA analysis was performed and each pair-wise comparison between control and experimental condition were made to obtain the *p* value (Levesque et al., 2006). Multiple hypothesis testing was accounted for by determining the False Discovery Rate (FDR or *q* value) for each comparison. A threshold of 2-fold expression changes with $q<0.001$ were considered to be highly significant.

Phenotypic analysis

Columbia-0 (Col-0 or wild type) and T-DNA insertion mutant seeds were surface sterilized either as described above, plated at a density of 16-20 seeds per plate (i.e. 8-10 control seeds and 8-10 mutant), and plates were wrapped in parafilm or porous tape. For direct germination, seeds were imbibed on standard or low Pi plates. For transfer experiments, seedlings were transferred to low Pi plates after 3 or 5 days on standard plates. Primary root lengths were marked daily and plates were scanned with a resolution of 800dpi at the end of each experiment (before roots touched the bottom of the plate). Root lengths were measured using ImageJ software (http://rsbweb.nih.gov/ij/). Emerged lateral roots were counted from these images as well. For quantification of meristem sizes, cortex cells were counted between the

quiescent center and first rapidly elongating cell. Numbers for the left file (when both files were counted) or the right file (when left was out of focus) of cortex cells were averaged and used for comparisons and statistics (student's TTest).

Cloning and transformation

Endogenous promoter regions (defined as the smaller of 3 kilobases upstream of the transcription start site or the region following an upstream gene's untranslated region) and coding sequences for genes of interest were PCR amplified from genomic DNA. TOPO TA cloning was used for promoters and TOPO-directional cloning for coding regions (Cat. #450641 and #K2435, respectively). For constitutive expression, the Ubiquitin 10 promoter (UBQ10) was used (GrassRoots Biotechnology). All transformations were carried out as described (doi:10.1038/nprot.2006.97).

3.2 Results and Discussion

Expression analysis

To gain a clearer understanding of root responses to Pi deprivation at the system level, we paired expression analysis with three tissue isolation approaches. First, a time-course to understand the dynamics of response and identify time-points relevant for future study revealed that within 48 hours of exposure, most transcript expression is repressed (Figure 5 and Appendix A, Figure 19A). Interestingly, most of the genes initially repressed after three hours had lower expression through the remaining time points. This suggests that shifts in regulatory processes may occur by three hours of

exposure. We reasoned that plants may down-regulate gene expression in an effort to free-up stored Pi resources for other uses. Strategically, this could aid in sustaining life through periods of nutrient deficiency allowing time to search for additional resources. Also, small transcriptional changes within this period could be meaningful, but perhaps are diluted out by homogenization of many tissues within the root. To gain an understanding of the roles of individual tissues, we used exposure of three hours for developmental zone-specific and tissue-specific transcriptional analyses.

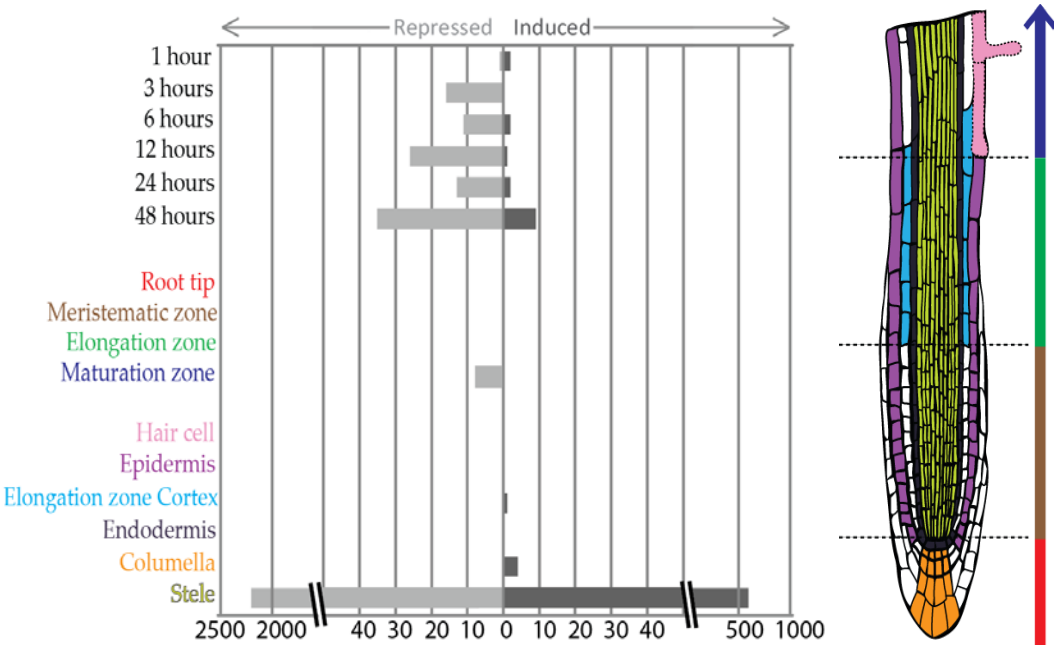

Figure 8: Total number of transcripts modulated. All genes induced (dark grey) and repressed (light grey) by 1.5-fold or greater (q<0.001) for each tissue type profiled. Root schematic shows developmental zones (arrow) and cell types isolated (colors).

With the aim of understanding the role of developmental stage in mediating low Pi-response, we profiled root tip (encompassing stem cell niche and root cap),

meristematic zone, elongation zone, and a section of the maturation/differentiation zone corresponding to the newly mature tissue. Our data indicate that mature tissue is most transcriptionally responsive, although a small number of genes are modulated. This suggests that, at this early exposure time-point, tissues may not become competent to respond until differentiated. Although few genes are modulated, eight are repressed specifically within the maturation zone, two of which are members of the purple acid phosphatase (PAP) family which has been implicated in P_i-deprivation response (Figure 5; Li et al., 2002). Interestingly, we found PAP8 to be repressed within mature root tissue after three hours while Li et al. found no change in PAP8 transcript level after 1, 3, and 5 days, highlighting a need for experiments with high spatial- and temporal-resolution.

The overall trend of reduced gene expression over time within the whole root is mirrored within the vascular tissue. We found that hair- and non-hair epidermis, elongating cortex, endodermis, and columella tissues do not alter their transcriptional programs significantly within three hours of low Pi. However, the stele tissue (root vasculature and pericycle) changes drastically by this time with many transcripts induced and many more repressed. This "–omics" level view of early events not only suggests that stele tissue is particularly responsive to Pi-deprivation, but that comparisons between whole organ and tissue-specific profiles can reveal quite a different perspective on the system as a whole. This result is surprising since the stele is

situated far from the soil interface and current descriptions of morphological alternations include additional root hair emergence close to the tip and transcriptional and physiological changes presumed to act at the root-soil interface (e.g. induction of high affinity Pi transporters and secreted phosphatases). However, the stele is mostly composed of vascular tissue which contains the xylem and phloem transport throughways that connect roots (location of Pi intake) with shoots (aerial portions of plants). With the overwhelming transcriptional response coming from the stele tissue, new questions arise about locations for P_i-sensing and signaling between root and shoot under these conditions. Interestingly, two of the genes induced here are SPX-domain containing transporters, which could suggest that P_i levels are monitored within these interior tissues. The SPX domain has been implicated in P_i homeostasis in *Saccharomyces cerevisiae* and is present in the low affinity P_i transporters Pho87 and Pho90 (Hurlimann et al., 2009). Follow-up on roles for these genes is needed because Pi sensing and signaling is likely to be complex in multicellular organisms such as plants. Our studies may shed light on the location of activity of many key players, something that only a system-level approach can provide in a high-throughput manner.

Hypothesizing that induced transcripts will more directly influence root response to this environmental insult, we focused on a sub-set of genes specifically induced in the stele (Supplemental Table 2). First, we asked whether these genes were expressed specifically in response to low Pi or if this was a generalized response to

deprivation of nutrients. Expression of these genes was compared to data for stele tissue following exposure to low sulfur (S) conditions for three hours. Interestingly, most genes are modulated in a low Pi-specific manner suggesting that this was not a general response to nutrient deprivation (Appendix A, Figure 19A). To find clues as to the significance of this gene-set, we looked for enrichment of gene ontology terms and found that genes specifically induced in the stele were enriched for signaling components and cell wall modifiers such as pectinesterases and lyases (Appendix A, Figure 19B).

Reverse genetics screen

We hypothesized that transcriptional modulation for developmental regulators would occur before overall primary root morphology is changed. Therefore, we used tissue-specific transcriptional data to ask whether genes specifically modulated in the vasculature can influence root development in response to low P_i. Due to significant enrichment for genes involved in signaling within vascular tissue, differentially expressed kinases were identified as candidates. We then screened insertional mutants of theses kinases for altered sensitivity to low P_i conditions. We found that one candidate mutant, *calcium-dependent protein kinase 24-1 (cpk24-1)*, was hypersensitive to low P_i with respect to primary root growth rate (Figure 9B; Alonso et al., 2003). This mutant contains a T-DNA insertion in the third of seven exons of the CPK24 gene, separating the calcium binding domain from the serine-threonine kinase and ATP-

binding domains, altering expression of the transcript (Figure 9A). According to qPCR results, exons downstream of the insertion are induced in the mutant, however the resulting protein is likely to be non-functional (not shown).

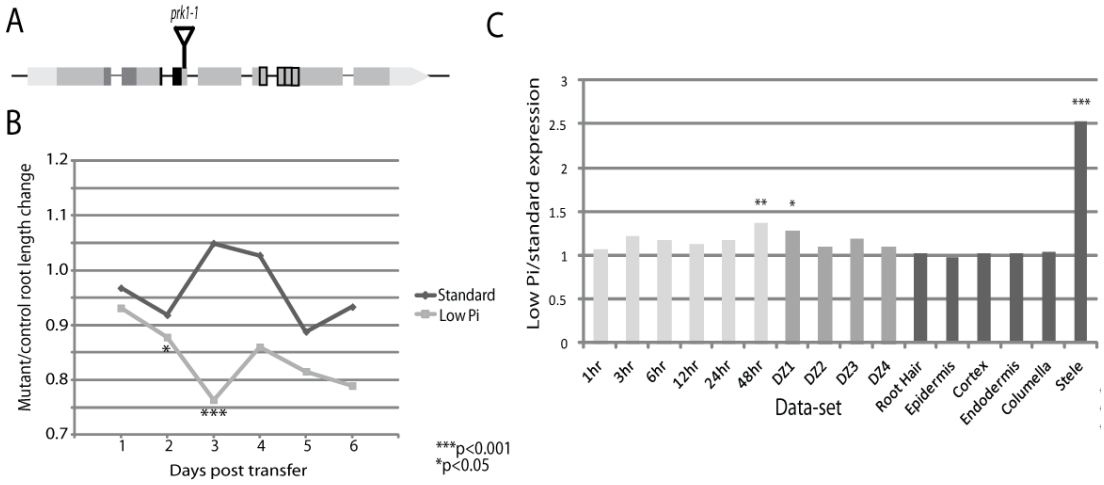

Figure 9: Candidate gene CPK24 is hypersensitive to Pi deprivation. (A) Schematic for CPK24 gene and T-DNA insertion site (*cpk24-1*). (B) Change in primary root over time expressed as ratios of mutant to wild type on standard (dark grey) and low Pi (Pi; light grey). *p<0.05 (C) Fold-change expression of CPK24 within whole roots (1hr-48hr), developmental zones (DZ1-4), and tissue types. ***p<0.001, **q<0.05, *p<0.1

For clues as to where in the vascular tissue CPK24 acts to alter root development in response to P_i-deprivation, we went back to the time-course and developmental zone-specific expression data. According to our time-course data, *CPK24* has a slight increase in expression after 3 hours on low Pi and highest expression after 48 hours. This could suggest that initial modulation of this gene is perpetuated when plants continue without P_i or that *CPK24* transcript increases over developmental time (Figure 9C). Additionally, after three hours on low P_i, slight increases in expression along the longitudinal axis lie

in the root tip and elongation zone, which highlighted these sites for further analysis. Next, we turned to previous work from the lab to confirm tissue-specificity. Comparisons between "RootMap" data and other abiotic stress data suggested that patterns of peak expression in standard conditions are enhanced in stress conditions (Dinneny et al., 2008; Iyer-Pascuzzi et al., 2011). The RootMap was constructed from expression profiles for isolated tissues and developmental sections of the Arabidopsis root under standard conditions (Brady et al., 2007). Therefore, we expected that peaks of *CPK24* expression in the RootMap will coincide with peaks of expression induction in low P_i data. This was true of *CPK24* expression as peaks of expression lie in the vascular tissue, specifically in the xylem, and root tip and elongation zone slices (Figure 9B and Appendix A, Figure 20). By *in silico* intersection, we infer that *CPK24* is specifically induced by low P_i within the root tip and elongating xylem. It is important to note that according to compilations of published transcriptomic studies, *CPK24* is specifically enriched in floral organs and seeds (Kilian et al., 2007). This suggests that roles for CPK24 in the root were below limits of detection when performing whole organ or whole plant analyses. To confirm that CPK24 is expressed in root vascular tissue, we expressed GFP under control of the endogenous *CPK24* promoter and found that expression is mostly excluded from meristematic tissues and is activated within vascular tissues of the elongation and differentiation zones in response to Pi-deprivation (Appendix A, Figures 21A and B). Surprisingly, expression was also found is epidermis

tissue, appearing to be specific to root hair lineages (Appendix A, Figure 21C). Our prediction is that CPK24 may control aspects of hair elongation as well as elongation of other tissues.

Based on evidence for CPK24 activity in root tip and elongating vascular tissues, we used confocal microscopy to observe low P_i-induced changes in root morphology. By 4DPT on low P_i (age 7DPI), the root apical meristem appears disorganized and the degree of disorganization grows over time. However, low-Pi induced disorganization in *cpk24-1* mutants appears similar to wild type (Appendix A, Figure 22). And, disorganization occurs within the same time-frame as wild type roots. Although this is a novel description of a morphological change in response to low P_i, this result suggests that CPK24 does not control this aspect of root morphogenesis. Additionally, based on the timing of meristem disorganization after four days, this morphological response is not, at least solely, responsible for the observed reduction in root growth rate in wild type plants which occurs after three days.

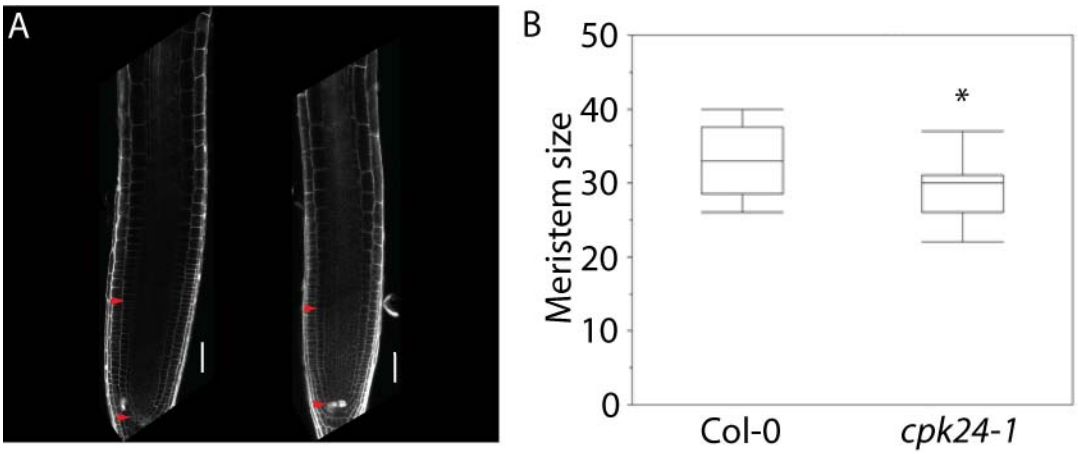

Figure 10: *cpk24-1* has a short meristem in low Pi conditions. (A) Longitudinal optical sections show meristem regions quantified (red arrowheads). Scale bars are 50uM in length. (B) Box plot represents three replicate experiments with meristem size reflected as number of cortex cells within regions in A. *p<0.05

According to our low P_i expression data, *CPK24* was slightly induced within the elongation zone (Figure 9C). This may suggest that CPK24 acts to modulate meristem size. So, we checked morphology in and around the elongation zone for Col-0 and *cpk24-1*, finding that meristems of wild type roots continued to grow in cell number over time and meristems of *cpk24-1*do not grow significantly over time (Appendix A, Figure 23). Furthermore, quantification of meristem sizes indicates that *cpk24-1*meristems are slightly, but significantly, shorter than wild type after four days of low P_i (Figures 10A and B). Taken together, these data suggest that we have identified a vascular-specific kinase that modulates meristem size under low P_i conditions to slow primary root growth, but it remains unclear whether CPK24 promotes meristem cell proliferation or represses transition of meristem cells from a proliferation program towards elongation.

After describing a novel feature of root response to low P_i, we asked whether *cpk24-1* roots were hypersensitive with respect to cell number and circumference length. Although we found *cpk24-1* to have no additional cortex, endodermis or pericycle cells relative to age-adjusted wild type roots (Appendix A, Figure 24), *cpk24-1* meristems are significantly larger in circumference by four days (Figure 11A). Additionally, the number of circumferential epidermal cells is significantly increased by two and four days on low P_i, further supporting a hypersensitive response to low P_i (Figure 11B). Interestingly, the earlier significant increase in epidermis cell number does not coincide with an increase in circumference length or number of other cell types in *cpk24-1* suggesting that epidermis divisions may precede these morphological changes in response to low Pi. This could mean that although the CPK24 transcript is modulated within the central cylinder of vascular cells, the gene product acts in external tissues to modulate root epidermis cell number and, perhaps indirectly, circumference.

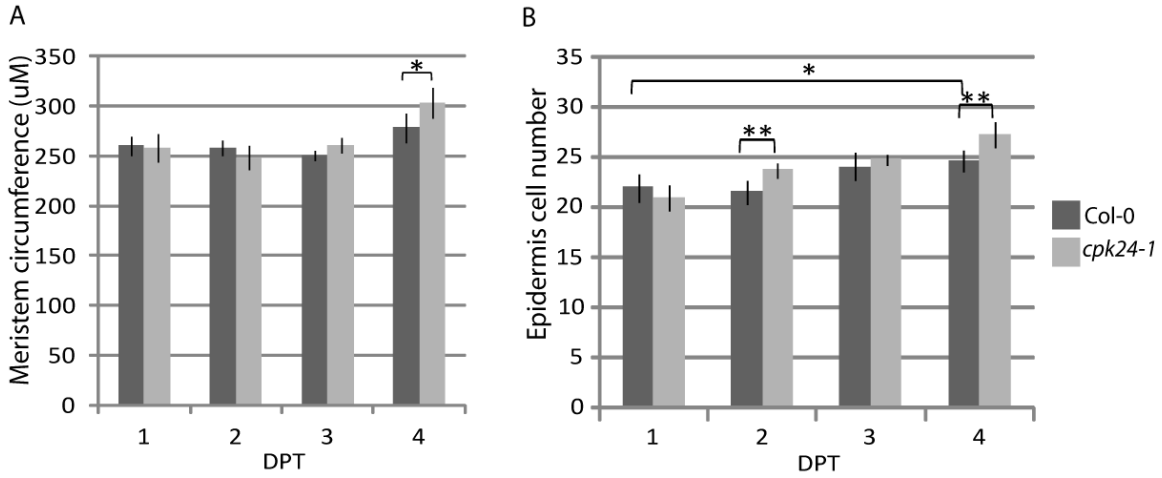

Figure 11: *cpk24-1* is hypersensitive to low Pi with respect to epidermis cell number and meristem circumference. (A) Transferred to low Pi at 3DPT, *cpk24-1* meristem circumference is larger than Col-0 wild type. (B) Although over time Col-0 exhibits an increase is circumferential cell number in response to low Pi, *cpk24-1* is hypersensitive and exhibits a larger increase after two and four days. **p<0.01, *p<0.05

Chapter 4. Bayesian Factor Analysis reveals transcriptional network for cell shape maintenance in response to salt stress

High-dimensional expression data-sets offer such a large amount of information that analyses often go unsaturated. Therefore, we combined published and unpublished data for responses to five stresses with respect to time, developmental stage, and root cell-type in an effort to uncover novel transcriptional networks influencing stress responses.

4.1 Methods

Expression data

All expression data for standard, low iron, high salt, low phosphate, acidic pH, and low sulfur conditions were normalized for array differences using Robust Multi-chip Averaging (RMA) followed by normalization to controls using Linear Models for Microarray data Analysis (LIMMA). Each condition included samples corresponding to 6-7 exposure time-points, 4 dissected developmental zones, and 5-6 cell types. From here, expression data for response to each stress condition within cell types were pulled out, filtered (2-fold change or greater and FDR<0.001 for two or more stresses), and analyzed using a Bayesian Factor Analysis model to yield co-expressed gene clusters/factors (Pruteanu-Malinici et al., 2011).

Quantitative RT-PCR

Microarray expression data was confirmed for 27 genes in cluster 3 using quantitative RT-PCR. Seedlings were transferred from standard to a selection of experimental conditions as described (1.5hours on 140mM NaCl, 3 hours on low Pi, and 24 hours on pH4.7). Controls for salt and phosphate were seedlings transferred from standard to standard conditions and roots harvested at 5DPI. Control for acidic pH was transferred from standard to standard and roots harvested at 6DPI. Each sample included pooled, whole root tissue from 4-5 plates (approximately 100 roots per sample). Samples were snap-frozen and RNA was prepared according to manufacturer's instructions for Qiagen Mini RNeasy kit.

4.2 Results and discussion

Expression data-sets and Bayesian Factor Analysis

Using a statistical Bayesian Factor Analysis approach, we found that unique expression patterns exist across tissues and stresses (Pruteanu-Malinici et al., 2011). Here, we analyzed expression clusters within single tissues, finding that one highly correlated gene cluster (cluster 3) emerged from vascular tissue data and included just 27 genes (Figure 12 and Appendix A, Figure 25). We hypothesized that genes within this cluster may be regulated by a tightly co-expressed transcription factor.

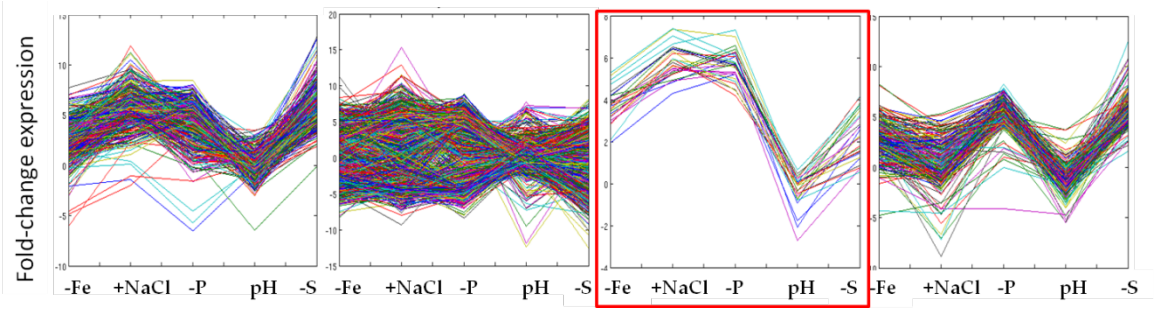

Figure 12: Gene clusters for vascular responses to five stress conditions. Factor analysis on stele-specific data for 5 stress conditions yielded 2,121 genes that met our filtering criteria of FDR<0.001 and >2fold change at two or more points. Cluster 3 of 4 (red box) revealed genes tightly coexpressed across conditions of iron deprivation (-Fe), high salt (+NaCl), phosphate deprivation (-P), acidic pH (pH), and sulfur deprivation (-S), including one transcription factor (SRTF1).

Stress responsive transcription factor and putative network for cell shape maintenance

We obtained a T-DNA insertional mutant for the single transcription factor found within cluster 3. We named the MYB-family transcription factor STRESS RESPONSIVE TRANSCRIPTION FACTOR1 (SRTF1). To elucidate roles for SRTF1 activity in response to abiotic stress, we measured growth rate under high salt, low phosphate, and acidic conditions. *srtf1-1* showed resistance to all three conditions after two days of exposure, and continued to grow better than wild type on low Pi and acidic media (Figure 13).

Upon finding that the disruption of *SRTF1* expression results in an early resistance to salt stress (i.e. within two days), we asked what the morphology of mutant roots looked like after exposure to salt within this time-frame. *srtf1-1* root meristems

appear normal when subjected to low levels of salt (Appendix A, Figure 26), but wild type roots respond to 140mM salt with swelling of cortex cells (Dinneny et al., 2008).

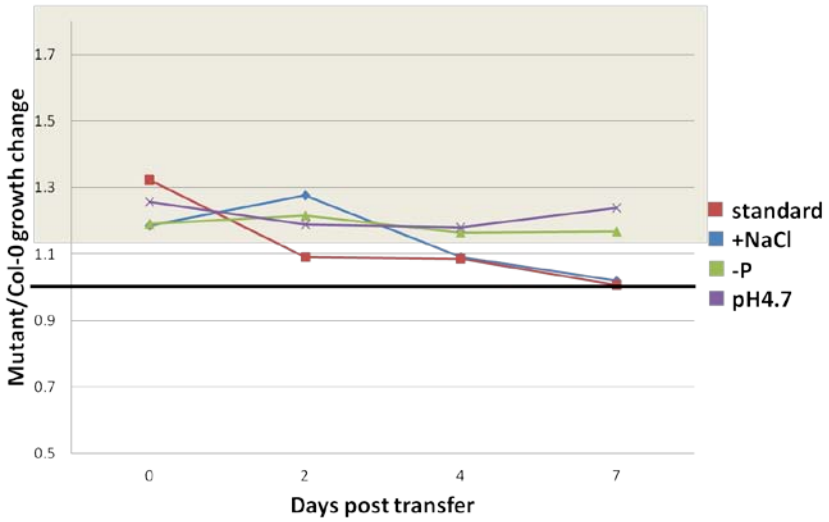

Figure 13: *srtf1-1* roots are resistant to stress. Ratios of mutant to wild type length change per day show that *srtf1-1* grows faster than wild type after 2 days on three stresses (+140mM NaCl in blue, low Pi in green, pH 4.7 in purple). Also, *srtf1-1* germinates sooner and/or grows faster than wild type according to standard growth rates at time of transfer (standard in red). Black line marks a ratio of 1, which would indicate equal growth rates. Shaded region includes statistically significant comparisons ($p<0.05$).

In an effort to identify SRTF1 target genes, we assayed expression levels for all co-expressed genes with mutant and wild type roots (cluster 3). Most putative targets showed no expression differences when treated with salt, low Pi or pH4.7 (Figures 14A and Appendix A, Figure 27). However, one gene, Expansin-like 3A (EXLA3), was specifically induced in response to salt within wild type and mutant roots (Figure 14A and Appendix A, Figure 28; Kilian et al., 2007). Interestingly, the degree of induction was higher in mutant roots suggesting that SRTF1 acts to repress or tune expression of

EXLA3 in response to salt. Although SRTF1 had not previously been characterized, others have shown that beyond the DNA-binding MYB domain, SRTF1 putatively binds to cytoskeletal components based on an *in vitro* screen for plant proteins that disrupt cell polarization in the yeast *Schizosaccharomyces pombe* (Xia et al., 1996). Taken together, these data support a model in which salt stress activates a cytoskeletal signal, perhaps through cellular swelling and an SRTF1 conformational change, which in turn activates SRTF1 protein activity to modulate transcription of *EXLA3* and other targets. As an expansin protein, EXLA3 could then act to maintain or modulate cell shape. Additionally, previous expression profiling of all root tissues suggests that *SRTF1* is transcribed within the phloem of root vasculature, and that putative target *EXLA3* is transcribed in adjacent tissues of the pericycle and endodermis (Figure 14B; Brady et al., 2007). This supports a model for SRTF1 as a non-cell autonomous transcription factor, which follows a mechanism for the root patterning regulator *SHORT-ROOT* (Helaruitta et al., 2000).

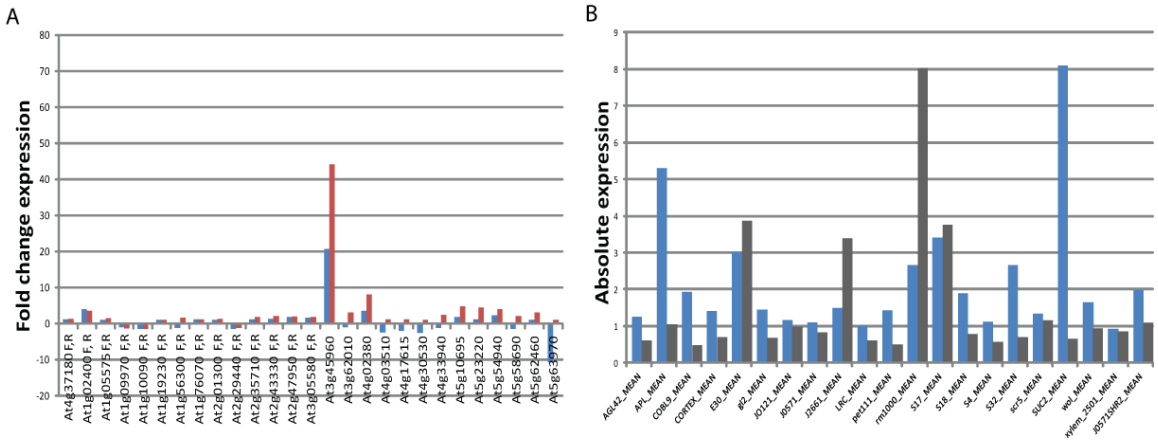

Figure 14: Expression of putative SRTF1 target genes. (A) Representative expression fold-change in +NaCl/standard conditions for wild type (blue) and *srtf1-1* (red). (B) Cell-type-specific expression data for *SRTF1* (blue) and *EXLA3* (grey) on standard conditions (Brady et al., 2007).

4.3 Future directions

After identifying a transcription factor that may bind to cytoskeletal proteins and modulates expression of an expansin-like protein in response to salt stress, my next steps are three-fold. First, I will replicate the phenotyping and expression experiments with an artificial microRNA against SRTF1 (sequence expressed by the constitutive promoter pUBQ10). This mutant construct will be transformed into the *pWOL:GFP* (wild-type) reporter background in order to repeat the expression study using vascular tissue that will have been isolated by FAC-sorting. Secondly, I will visualize expression localization of the transcript and protein. By cloning the endogenous promoter for SRTF1, I will express GFP under its control to confirm phloem-localized transcript expression. Also, I will clone the SRTF1 coding sequence and express a fusion with GFP under control of the endogenous promoter to understand whether the protein can move

between tissues to act. One possibility is that the protein will not translocate to its target nucleus until the root experiences salt stress. To explore this possibility, I will use cytoplasmic and nuclear markers to look for co-localization under standard and high salt conditions. Finally, the SRTF1-GFP protein fusion will be used to assay direct binding of SRTF1 protein to the EXLA3 promoter sequence. Using an anti-GFP antibody to precipitate fusion protein and target sequences, chromatin-immuno-precipitation (ChIP) followed by qPCR will be performed to verify binding to the *EXLA3* promoter.

Chapter 5. Conclusions and implications

Understanding root development is an important part of plant biology and developmental programs are highly dependent on environment conditions. Due to clear changes to root morphology in response to Pi-deprivation, we explored aspects of growth regulation to elucidate roles for individual tissues and to identify novel regulators.

Features of root developmental modulation had been described, but we narrowed down timing of two aspects to build a higher resolution description of these events. We found that primary roots grow at a significantly slower rate when subjected to an approximately 500-fold reduction of Pi-concentration after 3 days. Also, emerged root hair density is increased by this exposure time-point. We hypothesized that regulation underlying these morphological changes would be affected prior to this point in time. Therefore, we focused our studies prior to three days of exposure to elucidate early events in plant responses to P_i-deprivation.

In an effort to describe primary root responses with greater resolution, we examined many reporter lines and found that meristem disorganization and QC expansion occur by 2DPT. Additionally, we found that many cell types divide along a

division plane uncharacteristic of root development by 2DPT, resulting in significant increases to circumferential cell number and meristem circumference length. Mutations for the patterning regulator JKD, the microtubule severing protein ERH3, and the vacuolar sorting protein SHBY have been shown to phenocopy the cortex divisions observed, demonstrating that genetic control is likely (Webb et al., 2002; Hassan et al., 2010; Koizumi et al., 2013). For our current and future work, we will use expression analyses within dividing tissues and an EMS-mutagenesis screen for undivided cortex mutants to identify regulators of these divisions. We hypothesize that JKD, ERH3, and SHBY will be identified in this screen along with novel regulators. Based on the current model for root hair specification, timing of increased root hair emergence, and these data, we hypothesize that the functional outcome of an increase in circumferential cortex number is increased specification of root hair epidermal cells. And, we propose that these divisions of cortex cells result in increased uptake of Pi by enabling specification of additional root hairs. Interestingly, division responses were delayed in plants transferred to low Pi at an earlier age. We propose that divisions depend on hormone fluctuations that naturally occur during this period in growth. For future study, I would assay timing of low Pi-response divisions in the presence of cytokinin and gibberellin hormones. My prediction is that 3DPI roots will exhibit the division response earlier than 4DPT in the presence of cytokinin hormone, and that roots aged 5DPI will not divide after 2DPT on low Pi in the presence of gibberellin. The outcome of this simple

experiment will shed light on the interplay between hormones, genetic regulation and stress response in the context of development.

Beyond physical description of developmental modulation, we transcriptionally profiled roots from 1-48 hours of low Pi exposure, finding that most expression is down-regulated within this period. Although there is little overlap between our and others' results, we propose that plants may down-regulate expression initially to conserve resources and to modulate developmental programs within this time-period. Furthermore, we found that several genes modulated by 3 hours continued to be repressed at 48 hours, so we reasoned that early changes were important. Interestingly, individual tissue-type profiling revealed that within 3 hours, the vascular tissue is particularly responsive. From these data, we identified a kinase that is specifically induced within elongating root vascular tissue and influences meristem length and circumference in low Pi conditions. These results support the hypothesis that tissue type mediates response to Pi-deprivation, and that tightly controlled gene expression, both spatially and temporally, influences whole root growth.

For many reasons, several groups have studied and continue to study aspects of response to Pi-deprivation. We have added to this field by describing new aspects of root developmental modulation in response to Pi-deprivation. These features, along with tissue-specific expression data, will not only enable identification of new Pi-responsive genes, but also allow for elucidation of mechanisms controlling these cell

divisions. With this knowledge, we will better understand how roots acquire additional Pi resources at the root-soil interface allowing for design of more efficient plants.

Appendix A. Supplementary Figures

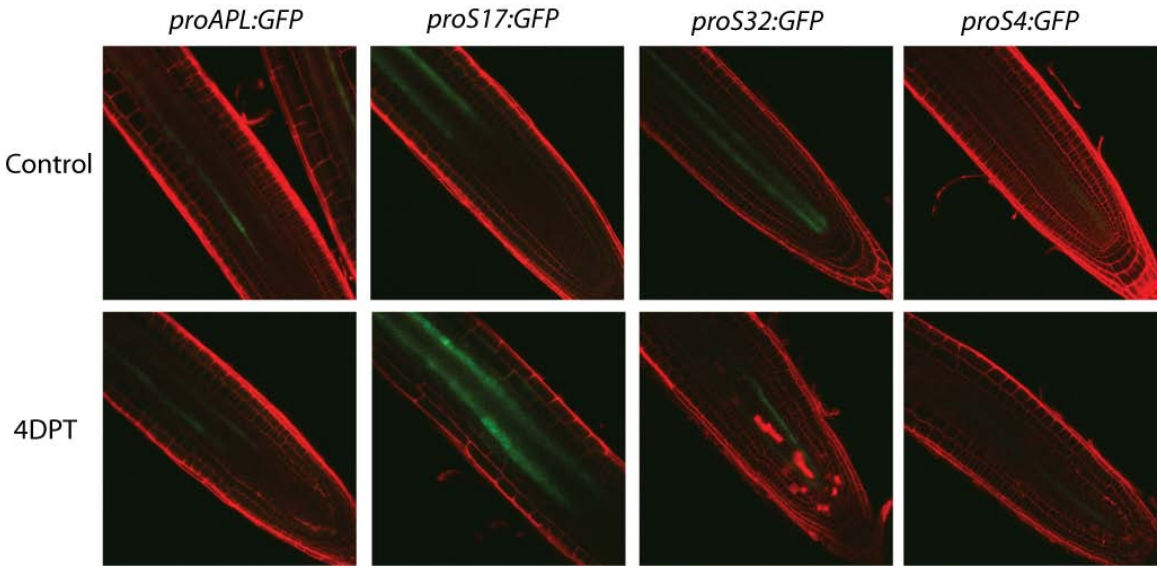

Figure 15: Vascular reporter expression on low Pi. GFP-reporters for phloem (*proAPL:GFP* and *proS17:GFP*) and xylem (*proS32:GFP* and *proS4:GFP*) show no change in expression pattern under low Pi conditions.

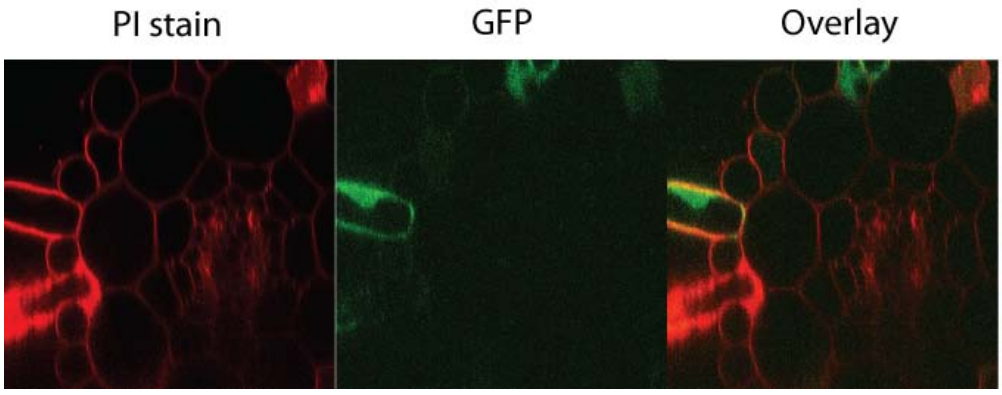

Figure 16: Ectopic root hair emergence. Transverse optical section of *pCOBL9:GFP* reporter root after four days on low Pi showing root hair outgrowth at cortex cell junction (lower hair) and directly over a cortex cell (upper hair).

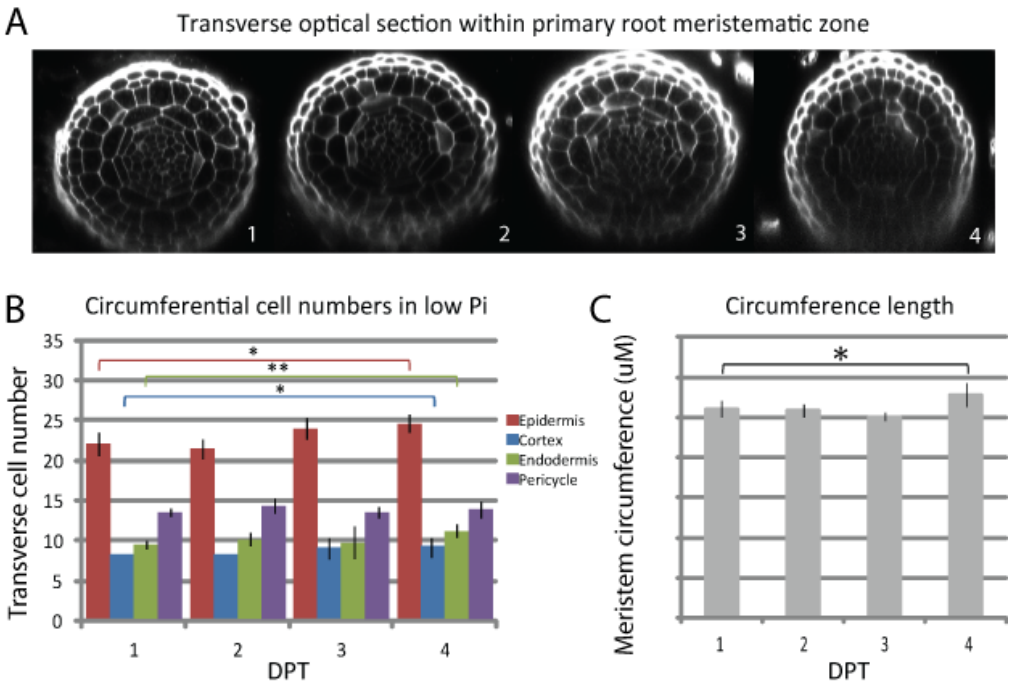

Figure 17: Early transfer delays Col-0 response to low Pi. (A) Transverse optical sections of three day old roots transferred to low Pi for 1-4 days. (B) Circumferential cell quantification shows significant increases to epidermis, cortex, and endodermis cell numbers by 4DPT, but no change in pericycle cell number. (C) Meristem circumference length significantly increased by 4DPT. **p<0.01, *p<0.05

Table 1: All genes induced by 2-fold or greater over control in response to low Pi in *pCO2:YFP-H2A* time-course.

AGI	Gene Description	Time(s) of induction
At1g48920	ATNUC-L1, NUC-L1, PARL1, nucleolin like 1	24h, 36h, 48h
At1g52190	Major facilitator superfamily protein	24h, 36h
At1g54970	ATPRP1, PRP1, RHS7, proline-rich protein 1	24h, 48h
At1g56110	NOP56, homolog of nucleolar protein NOP56	24h, 36h, 48h
At1g56680	Chitinase family protein	24h
At1g65570	Pectin lyase-like superfamily protein	24h, 36h
At1g73620	Pathogenesis-related thaumatin superfamily protein	24h, 36h, 48h
At2g04025	RGF3, Encodes a root meristem growth factor (RGF).	24h, 48h
At2g21660	ATGRP7, CCR2, GR-RBP7, GRP7, cold, circadian rhythm, and rna binding 2	24h, 36h, 48h
At2g29500	HSP20-like chaperones superfamily protein	24h
At3g18130	RACK1C_AT, receptor for activated C kinase 1C	24h, 36h, 48h
At3g44750	ATHD2A, HD2A, HDA3, HDT1, histone deacetylase 3	24h, 36h, 48h
At3g44990	ATXTR8, XTH31, XTR8, xyloglucan endo-transglycosylase-related 8	24h
At3g57150	AtCBF5, AtNAP57, CBF5, NAP57, homologue of NAP57	24h, 36h
At4g25630	ATFIB2, FIB2, fibrillarin 2	24h, 36h, 48h
At4g38680	ATCSP2, CSDP2, CSP2, GRP2, glycine rich protein 2	24h, 36h
At5g22580	Stress responsive A/B Barrel Domain	24h, 48h
At5g52640	ATHS83, AtHsp90-1, ATHSP90.1, heat shock protein 90.1	24h
At5g57530	AtXTH12, XTH12, xyloglucan endotransglucosylase/hydrolase 12	24h, 48h
At1g18250	ATLP-1, Pathogenesis-related thaumatin superfamily protein	36h, 48h
At1g29980	Protein of unknown function, DUF642	36h
At1g54690	G-H2AX, GAMMA-H2AX, H2AXB, HTA3, gamma histone variant H2AX	36h, 48h
At1g71380	ATCEL3, ATGH9B3, CEL3, cellulase 3	36h, 48h
At1g73780	Bifunctional inhibitor/lipid-transfer protein/seed storage 2S albumin superfamily protein	36h, 48h
At2g28790	Pathogenesis-related thaumatin superfamily protein	36h, 48h
At3g23830	GR-RBP4, GRP4, glycine-rich RNA-binding protein 4	36h, 48h
At3g47420	ATPS3, PS3, phosphate starvation-induced gene 3	36h
At3g56070	ROC2, rotamase cyclophilin 2	36h, 48h
At4g12600	Ribosomal protein L7Ae/L30e/S12e/Gadd45 family protein	36h, 48h
At4g13850	ATGRP2, GR-RBP2, GRP2, glycine-rich RNA-binding protein 2	36h, 48h
At4g24780	Pectin lyase-like superfamily protein	36h
At4g26880	Stigma-specific Stig1 family protein	36h, 48h
At4g31840	AtENODL15, ENODL15, early nodulin-like protein 15	36h, 48h
At4g38410	Dehydrin family protein	36h, 48h
At4g39800	ATIPS1, ATMIPS1, MI-1-P SYNTHASE, MIPS1, myo-inositol-1-phosphate synthase 1	36h
At5g03960	IQD12, IQ-domain 12	36h
At5g05270	Chalcone-flavanone isomerase family protein	36h, 48h
At5g20150	ATSPX1, SPX1, SPX domain gene 1	36h, 48h
At5g22650	ATHD2, ATHD2B, HD2, HD2B, HDA4, HDT02, HDT2, histone deacetylase 2B	36h, 48h
At5g51520	Plant invertase/pectin methylesterase inhibitor superfamily protein	36h
At5g57770	Plant protein of unknown function (DUF828) with plant pleckstrin homology-like region	36h
At1g02870	FUNCTIONS IN: molecular_function unknown	48h
At1g04480	Ribosomal protein L14p/L23e family protein	48h
At1g07070	Ribosomal protein L35Ae family protein	48h
At1g08580	unknown protein	48h
At1g18540	Ribosomal protein L6 family protein	48h
At1g22780	PFL, PFL1, RPS18A, Ribosomal protein S13/S18 family	48h
At1g23410	Ribosomal protein S27a / Ubiquitin family protein	48h

AGI	Gene Description	Time(s) of induction
At1g25260	Ribosomal protein L10 family protein	48h
At1g26880	Ribosomal protein L34e superfamily protein	48h
At1g27400	Ribosomal protein L22p/L17e family protein	48h
At1g29250	Alba DNA/RNA-binding protein	48h
At1g29270	unknown protein	48h
At1g31970	STRS1, DEA(D/H)-box RNA helicase family protein	48h
At1g33280	ANAC015, BRN1, NAC015, NAC domain containing protein 15	48h
At1g46264	AT-HSFB4, HSFB4, SCZ, heat shock transcription factor B4	48h
At1g48630	RACK1B_AT, receptor for activated C kinase 1B	48h
At1g50920	Nucleolar GTP-binding protein	48h
At1g52930	Ribosomal RNA processing Brix domain protein	48h
At1g61570	TIM13, translocase of the inner mitochondrial membrane 13	48h
At1g69700	ATHVA22C, HVA22C, HVA22 homologue C	48h
At1g72370	AP40, P40, RP40, RPSAA, 40s ribosomal protein SA	48h
At1g74500	ATBS1, BS1, TMO7, activation-tagged BRI1(brassinosteroid-insensitive 1)-suppressor 1	48h
At1g80270	PPR596, PENTATRICOPEPTIDE REPEAT 596	48h
At1g80750	Ribosomal protein L30/L7 family protein	48h
At2g01250	Ribosomal protein L30/L7 family protein	48h
At2g14460	unknown protein	48h
At2g19730	Ribosomal L28e protein family	48h
At2g19750	Ribosomal protein S30 family protein	48h
At2g20450	Ribosomal protein L14	48h
At2g20490	EDA27, NOP10, nucleolar RNA-binding Nop10p family protein	48h
At2g21580	Ribosomal protein S25 family protein	48h
At2g23050	NPY4, Phototropic-responsive NPH3 family protein	48h
At2g23410	ACPT, CPT, cis-prenyltransferase	48h
At2g23930	SNRNP-G, probable small nuclear ribonucleoprotein G	48h
At2g25210	Ribosomal protein L39 family protein	48h
At2g27190	ATPAP1, ATPAP12, PAP1, PAP12, purple acid phosphatase 12	48h
At2g27840	HDA13, HDT04, HDT4, histone deacetylase-related / HD-related	48h
At2g32060	Ribosomal protein L7Ae/L30e/S12e/Gadd45 family protein	48h
At2g33370	Ribosomal protein L14p/L23e family protein	48h
At2g34480	Ribosomal protein L18ae/LX family protein	48h
At2g35605	SWIB/MDM2 domain superfamily protein	48h
At2g36620	RPL24A, ribosomal protein L24	48h
At2g37190	Ribosomal protein L11 family protein	48h
At2g39460	ATRPL23A, RPL23A, RPL23AA, ribosomal protein L23AA	48h
At2g39700	ATEXP4, ATEXPA4, ATHEXP ALPHA 1.6, EXPA4, expansin A4	48h
At2g40360	Transducin/WD40 repeat-like superfamily protein	48h
At2g41650	unknown protein	48h
At2g42740	RPL16A, ribosomal protein large subunit 16A	48h
At2g44120	Ribosomal protein L30/L7 family protein	48h
At2g44860	Ribosomal protein L24e family protein	48h
At2g45860	unknown protein	48h
At2g47610	Ribosomal protein L7Ae/L30e/S12e/Gadd45 family protein	48h
At3g02530	TCP-1/cpn60 chaperonin family protein	48h
At3g03920	H/ACA ribonucleoprotein complex, subunit Gar1/Naf1 protein	48h
At3g04840	Ribosomal protein S3Ae	48h
At3g05060	NOP56-like pre RNA processing ribonucleoprotein	48h
At3g05560	Ribosomal L22e protein family	48h
At3g05590	RPL18, ribosomal protein L18	48h
At3g06680	Ribosomal L29e protein family	48h

AGI	Gene Description	Time(s) of induction
At3g07110	Ribosomal protein L13 family protein	48h
At3g10090	Nucleic acid-binding, OB-fold-like protein	48h
At3g10610	Ribosomal S17 family protein	48h
At3g13230	RNA-binding KH domain-containing protein	48h
At3g13580	Ribosomal protein L30/L7 family protein	48h
At3g14600	Ribosomal protein L18ae/LX family protein	48h
At3g15357	unknown protein	48h
At3g16080	Zinc-binding ribosomal protein family protein	48h
At3g16780	Ribosomal protein L19e family protein	48h
At3g18600	P-loop containing nucleoside triphosphate hydrolases superfamily protein	48h
At3g18740	Ribosomal protein L7Ae/L30e/S12e/Gadd45 family protein	48h
At3g22230	Ribosomal L27e protein family	48h
At3g23390	Zinc-binding ribosomal protein family protein	48h
At3g27060	ATTSO2, TSO2, Ferritin/ribonucleotide reductase-like family protein	48h
At3g44590	60S acidic ribosomal protein family	48h
At3g46040	RPS15AD, ribosomal protein S15A D	48h
At3g46560	emb2474, TIM9, Tim10/DDP family zinc finger protein	48h
At3g48930	EMB1080, Nucleic acid-binding, OB-fold-like protein	48h
At3g49010	ATBBC1, BBC1, RSU2, breast basic conserved 1	48h
At3g49190	O-acyltransferase (WSD1-like) family protein	48h
At3g51800	ATEBP1, ATG2, EBP1, metallopeptidase M24 family protein	48h
At3g52580	Ribosomal protein S11 family protein	48h
At3g53190	Pectin lyase-like superfamily protein	48h
At3g53430	Ribosomal protein L11 family protein	48h
At3g53890	Ribosomal protein S21e	48h
At3g55280	RPL23AB, ribosomal protein L23AB	48h
At3g56340	Ribosomal protein S26e family protein	48h
At3g58610	ketol-acid reductoisomerase	48h
At3g58660	Ribosomal protein L1p/L10e family	48h
At3g58700	Ribosomal L5P family protein	48h
At3g60770	Ribosomal protein S13/S15	48h
At3g61110	ARS27A, RS27A, ribosomal protein S27	48h
At3g61930	unknown protein	48h
At3g62760	ATGSTF13, Glutathione S-transferase family protein	48h
At4g03210	XTH9, xyloglucan endotransglucosylase/hydrolase 9	48h
At4g09320	NDPK1, Nucleoside diphosphate kinase family protein	48h
At4g10450	Ribosomal protein L6 family	48h
At4g10480	Nascent polypeptide-associated complex (NAC), alpha subunit family protein	48h
At4g14320	Zinc-binding ribosomal protein family protein	48h
At4g14690	ELIP2, Chlorophyll A-B binding family protein	48h
At4g15770	RNA binding	48h
At4g15910	ATDI21, DI21, drought-induced 21	48h
At4g16720	Ribosomal protein L23/L15e family protein	48h
At4g17390	Ribosomal protein L23/L15e family protein	48h
At4g17520	Hyaluronan / mRNA binding family	48h
At4g19460	UDP-Glycosyltransferase superfamily protein	48h
At4g23800	HMG (high mobility group) box protein	48h
At4g23920	ATUGE2, UGE2, UDP-D-glucose/UDP-D-galactose 4-epimerase 2	48h
At4g25340	ATFKBP53, FKBP53, FK506 BINDING PROTEIN 53	48h
At4g25740	RNA binding Plectin/S10 domain-containing protein	48h
At4g25890	60S acidic ribosomal protein family	48h
At4g26230	Ribosomal protein L31e family protein	48h

AGI	Gene Description	Time(s) of induction
At4g29410	Ribosomal L28e protein family	48h
At4g30800	Nucleic acid-binding, OB-fold-like protein	48h
At4g31500	ATR4, CYP83B1, RED1, RNT1, SUR2, cytochrome P450, family 83, subfamily B	48h
At4g31985	Ribosomal protein L39 family protein	48h
At4g34670	Ribosomal protein S3Ae	48h
At4g39950	CYP79B2, cytochrome P450, family 79, subfamily B, polypeptide 2	48h
At5g02050	Mitochondrial glycoprotein family protein	48h
At5g02490	Heat shock protein 70 (Hsp 70) family protein	48h
At5g02610	Ribosomal L29 family protein	48h
At5g06360	Ribosomal protein S8e family protein	48h
At5g08180	Ribosomal protein L7Ae/L30e/S12e/Gadd45 family protein	48h
At5g09510	Ribosomal protein S19 family protein	48h
At5g10400	Histone superfamily protein	48h
At5g14520	pescadillo-related	48h
At5g15520	Ribosomal protein S19e family protein	48h
At5g15750	Alpha-L RNA-binding motif/Ribosomal protein S4 family protein	48h
At5g16130	Ribosomal protein S7e family protein	48h
At5g20160	Ribosomal protein L7Ae/L30e/S12e/Gadd45 family protein	48h
At5g20890	TCP-1/cpn60 chaperonin family protein	48h
At5g20950	Glycosyl hydrolase family protein	48h
At5g22440	Ribosomal protein L1p/L10e family	48h
At5g22880	H2B, HTB2, histone B2	48h
At5g23740	RPS11-BETA, ribosomal protein S11-beta	48h
At5g27850	Ribosomal protein L18e/L15 superfamily protein	48h
At5g28640	AN3, ATGIF1, GIF, GIF1, SSXT family protein	48h
At5g39740	OLI7, RPL5B, ribosomal protein L5 B	48h
At5g47210	Hyaluronan / mRNA binding family	48h
At5g48760	Ribosomal protein L13 family protein	48h
At5g52470	ATFBR1, ATFIB1, FBR1, FIB1, SKIP7, fibrillarin 1	48h
At5g52920	PKP-BETA1, PKP1, PKP2, plastidic pyruvate kinase beta subunit 1	48h
At5g55920	OLI2, S-adenosyl-L-methionine-dependent methyltransferases superfamily protein	48h
At5g56710	Ribosomal protein L31e family protein	48h
At5g57500	Galactosyltransferase family protein	48h
At5g58420	Ribosomal protein S4 (RPS4A) family protein	48h
At5g59850	Ribosomal protein S8 family protein	48h
At5g59870	HTA6, histone H2A 6	48h
At5g60670	Ribosomal protein L11 family protein	48h
At5g61020	ECT3, evolutionarily conserved C-terminal region 3	48h
At5g61170	Ribosomal protein S19e family protein	48h
At5g62190	PRH75, DEAD box RNA helicase (PRH75)	48h
At5g64080	Bifunctional inhibitor/lipid-transfer protein/seed storage 2S albumin superfamily protein	48h
At5g64140	RPS28, ribosomal protein S28	48h
At5g65360	Histone superfamily protein	48h
At5g67360	ARA12, Subtilase family protein	48h
At5g67510	Translation protein SH3-like family protein	48h

Table 2: All genes induced by 2-fold or greater over control in response to low Pi in *pWER:GFP* time-course.

AGI	Gene Description	Time(s) of induction
At2g04460	transposable element gene	24h, 48h
At3g47420	ATPS3, PS3, phosphate starvation-induced gene 3	24h, 48h
At5g20150	ATSPX1, SPX1, SPX domain gene 1	24h, 48h
At5g20790	unknown protein	24h, 48h
At1g23210	AtGH9B6, GH9B6, glycosyl hydrolase 9B6	36h
At1g33700	Beta-glucosidase, GBA2 type family protein	36h, 48h
At1g34510	Peroxidase superfamily protein	36h, 48h
At1g54970	ATPRP1, PRP1, RHS7, proline-rich protein 1	36h, 48h
At1g56680	Chitinase family protein	36h
At2g01530	MLP329, MLP-like protein 329	36h, 48h
At2g04025	RGF3, Encodes a root meristem growth factor (RGF).	36h
At2g20520	FLA6, FASCICLIN-like arabinogalactan 6	36h, 48h
At2g30860	ATGSTF7, ATGSTF9, GLUTTR, GSTF9, glutathione S-transferase PHI 9	36h
At3g02870	VTC4, Inositol monophosphatase family protein	36h
At3g49960	Peroxidase superfamily protein	36h, 48h
At3g60330	AHA7, HA7, H(+)-ATPase 7	36h, 48h
At4g26260	MIOX4, myo-inositol oxygenase 4	36h, 48h
At5g04960	Plant invertase/pectin methylesterase inhibitor superfamily	36h, 48h
At5g22410	RHS18, root hair specific 18	36h, 48h
At5g57530	AtXTH12, XTH12, xyloglucan endotransglucosylase/hydrolase 12	36h, 48h
At5g57540	AtXTH13, XTH13, xyloglucan endotransglucosylase/hydrolase 13	36h, 48h
At5g67400	RHS19, root hair specific 19	36h, 48h
At1g01750	ADF11, actin depolymerizing factor 11	48h
At1g12950	RSH2, root hair specific 2	48h
At1g23140	Calcium-dependent lipid-binding (CaLB domain) family protein	48h
At1g62980	ATEXP18, ATEXPA18, ATHEXP ALPHA 1.25, EXP18, EXPA18, expansin A18	48h
At1g78370	ATGSTU20, GSTU20, glutathione S-transferase TAU 20	48h
At2g01880	ATPAP7, PAP7, purple acid phosphatase 7	48h
At2g25240	Serine protease inhibitor (SERPIN) family protein	48h
At2g46860	AtPPa3, PPa3, pyrophosphorylase 3	48h
At3g02040	SRG3, senescence-related gene 3	48h
At3g10710	RHS12, root hair specific 12	48h
At3g52190	PHF1, phosphate transporter traffic facilitator1	48h
At3g62680	ATPRP3, PRP3, proline-rich protein 3	48h
At4g25820	ATXTH14, XTH14, XTR9, xyloglucan endotransglucosylase/hydrolase 14	48h
At4g30670	Putative membrane lipoprotein	48h
At4g33030	SQD1, sulfoquinovosyldiacylglycerol 1	48h
At4g33730	Cysteine-rich secretory proteins, Antigen 5, and Pathogenesis-related 1 protein	48h
At4g40090	AGP3, arabinogalactan protein 3	48h
At5g35190	proline-rich extensin-like family protein	48h

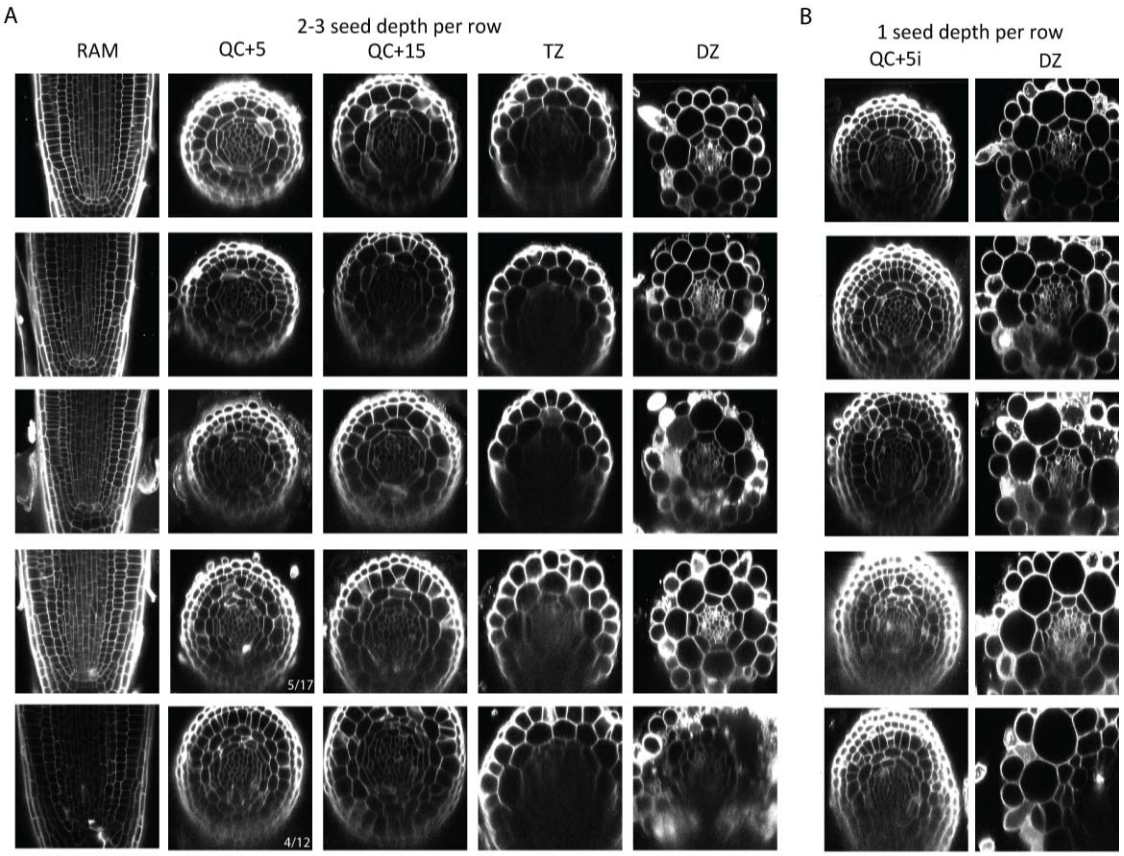

Figure 18: Dense plating delays response to low Pi. (A) Cortex divisions delayed to 4DPT with densely plated seed (4th row), occurring in approximately 30% of roots. (B) Cortex divisions occur in all roots at 2DPT with 1 seed depth per row (3rd row)

Table 3: Candidate genes for reverse genetics screen.

AGI	Data-set	Mutant line	Phenotypes screened
A1g32870	1h, 3h, 6h, 12h, 24h, 48h	Salk096150	Growth rate, lateral root density
At1g05180	Root hair network	Salk_143810, Salk_141487, Salk_039256	Growth rate, lateral root density
At1g20880	WOL	SALK 035511	Growth rate, meristem length
At1g22985	6h, 12h	Salk023227	Growth rate, lateral root density
At1g31050	SCR2.0	SALK 095172, SALK 065747	Growth rate, lateral root density
At1g62150	WOL	SALK 022625	Growth rate, lateral root density
At1g70370	COR315.1	Salk090053	Growth rate, lateral root density
At1g70690	48h	Salk_016278	Growth rate, lateral root density
At1g74660	LZ4	Salk038432	Growth rate, lateral root density
At1g76370	WOL	SALK_045159	Growth rate, lateral root density
At1g76800	12h	SALK 060224	Growth rate, lateral root density
At2g07040	WOL	SALK_110653	Growth rate, lateral root density
At2g17560	WOL	SALK 133100	Growth rate, lateral root density
At2g20560	PET111	Salk 113356	Growth rate, lateral root density
At2g22475	Root hair network	Salk_015291	Growth rate, lateral root density
At2g31500	WOL	SALK 015986	Growth rate, lateral root density, meristem cell composition and circumference, meristem length, meristem organization
At2g33480	1h, 3h, 12h	Salk_066378	Growth rate, lateral root density
At2g34710	WOL	SALK 008924	Growth rate, lateral root density
At2g46240	PET111	Salk 004760	Growth rate, lateral root density
At2g46670	WOL	Salk086222	Growth rate, lateral root density
At3g04130	PET111	SALK_008824	Growth rate, lateral root density
AT3G09350	PET111	SALK_021784, SALK_050697	Growth rate, lateral root density
At3g09360	WOL	SALK 050697	Growth rate, lateral root density
At3g25250	24h, 48h	Salk_135617	Growth rate, lateral root density
At3g50260	WOL	Salk071613	Growth rate, lateral root density, meristem organization
AT3G53230	48h, PET111	SALK 005957	Growth rate, lateral root density, meristem length
At4g01250	1h	SALK 098205	Growth rate, lateral root density
At4g04960	12h	Salk_045505, Salk_045506, Salk_016807	Growth rate, lateral root density
At4g12400	PET111	SALK 023494	Growth rate, lateral root density
AT4G23750	WOL	SALK 021613	Growth rate, lateral root density
At4g32880	WOL	SALK 023733	Growth rate, lateral root density, meristem organization
At5g10510	WOL	SALK 021823	Growth rate, lateral root density
At5g13080	WOL	SALK 101367	Growth rate, lateral root density
At5g13680	WOL	SALK 005153	Growth rate, lateral root density
At5g14750	WOL	Salk_114008	Growth rate, lateral root density
At5g16600	SCR2.0	SALK 030146	Growth rate, lateral root density
At5g51440	24h	Salk 118536	Growth rate, lateral root density
At5g61590	WOL	SALK 015182	Growth rate, lateral root density

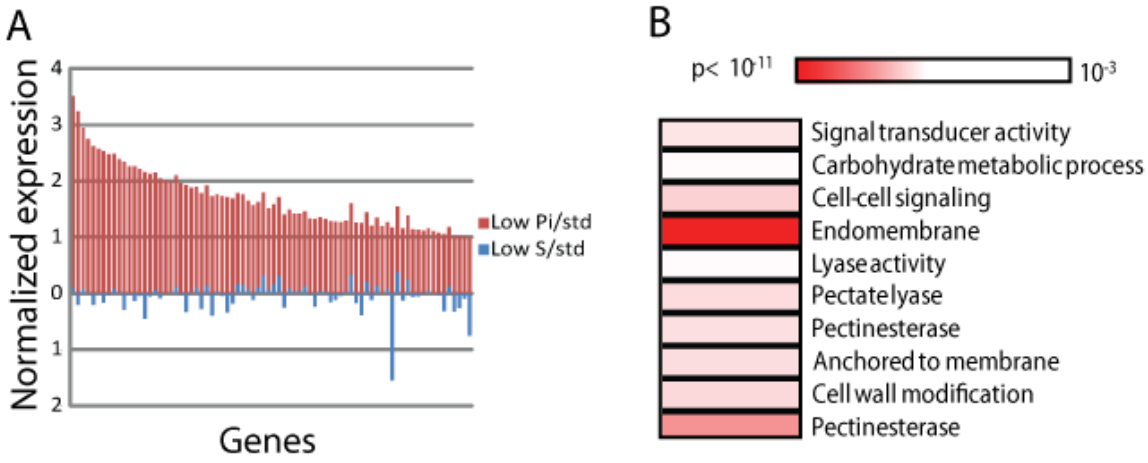

Figure 19: Genes induced within stele tissue. (A) Expression induction specific to low Pi (red) when compared to low sulfur (S; blue). (B) Significantly enriched gene ontology categories for low Pi-induced genes within stele.

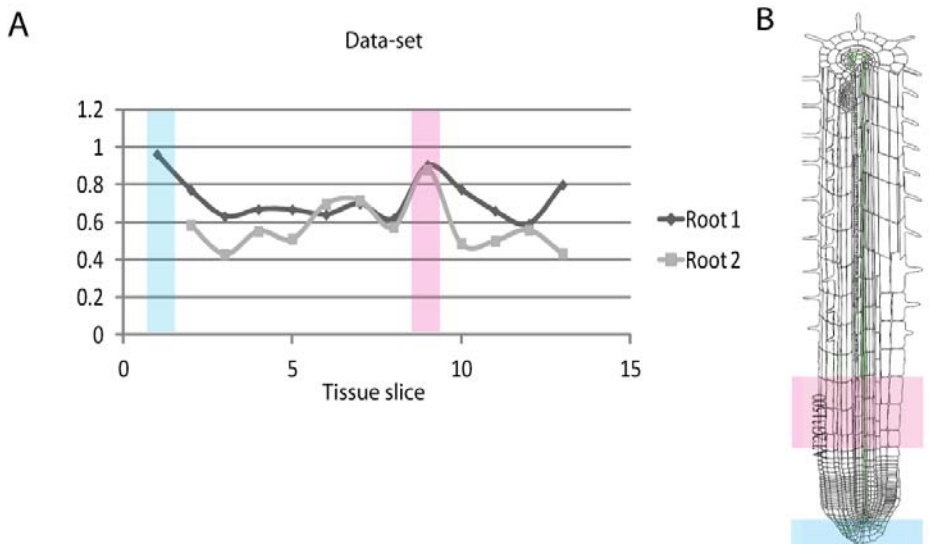

Figure 20: RootMap expression for CPK24. (A) Longitudinal sections show CPK24 transcript peaks in the root tip (light blue) and elongation zone (pink) slices. (B) Cell-type profiling shows CPK24 expression is highest within the vascular tissue (light green).

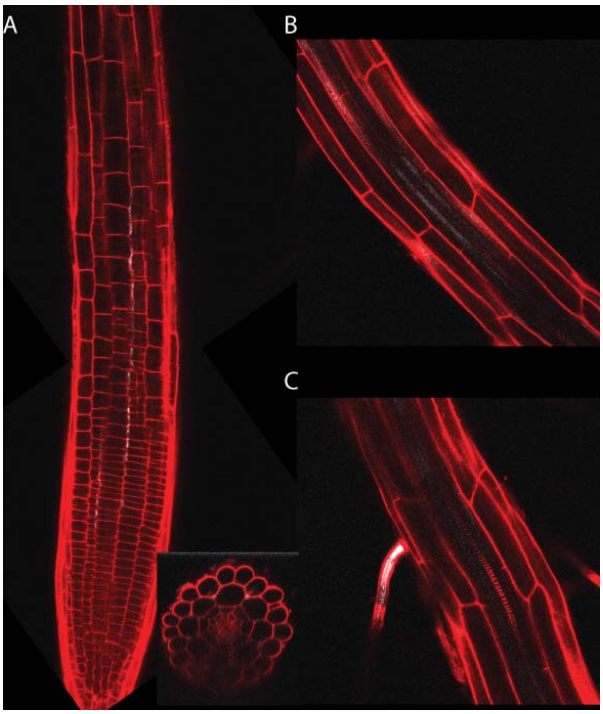

Figure 21: *pCPK24:GFP-ER* reporter expression. (A) Meristematic tissues exhibit no ER-localized GFP, but, likely non-specifically, GFP accumulates between cells of the cortex and epidermis (white). (B) In standard conditions, expression is observed in elongation zone vascular and epidermis tissues. (C) After 24 hours in low Pi conditions, *pCPK24:GFP-ER* is expressed in non-xylem vascular tissue and root hair epidermis. Red counter-stain is propidium iodide.

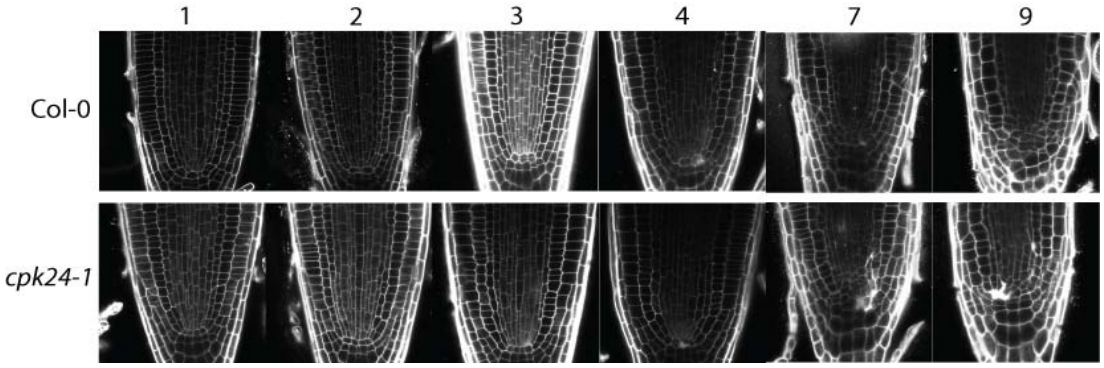

Figure 22: Low Pi-induced meristem disorganization occurs no earlier in *cpk24-1* than Col-0.

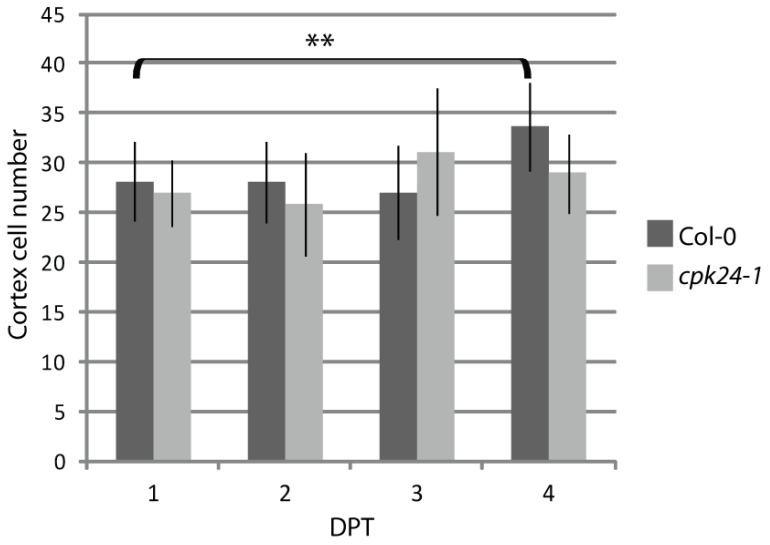

Figure 23: Low Pi causes increase in meristem size over time. Col-0 exhibits an increase in meristem size by 4DPT (dark grey; transfer at 3DPI). *cpk24-1* exhibits no significant change to meristem size (light grey). **p<0.01

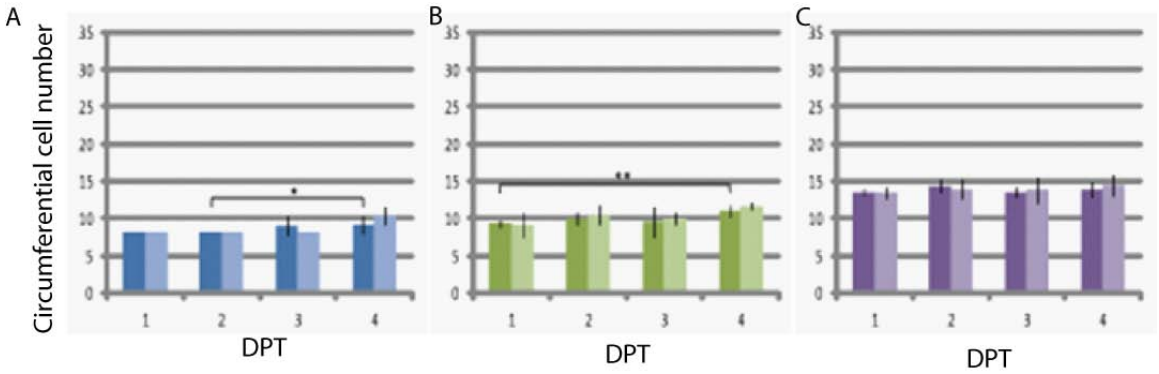

Figure 24: *cpk24-1* no different than Col-0. Col-0 (dark shade) and *cpk24-1* (light shade) have no difference in cortex- (A), endodermis- (B), or pericycle- (C) cell numbers after 4 days on low Pi.

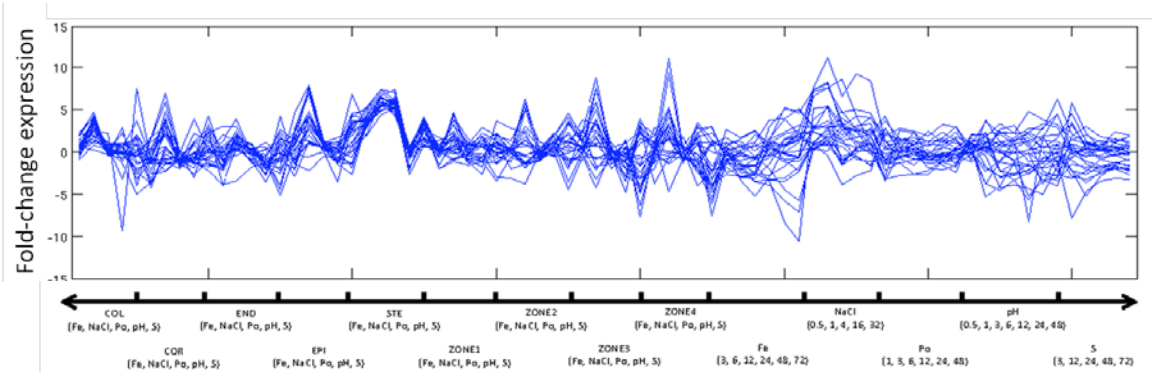

Figure 25: Concatenated expression for cluster 3. All cell type (Col, Cor, End, Epi, and Ste), developmental zone (Zones 1-4), and time-course (Fe, NaCl, P, pH, and S) expression data for cluster 3 genes shows increased agreement within tissues isolated at higher spatial resolution.

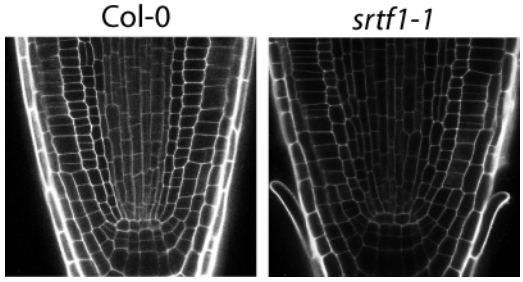

Figure 26: *srtf1-1* root tip organization is normal. Roots were treated with 25mM NaCl for 24h.

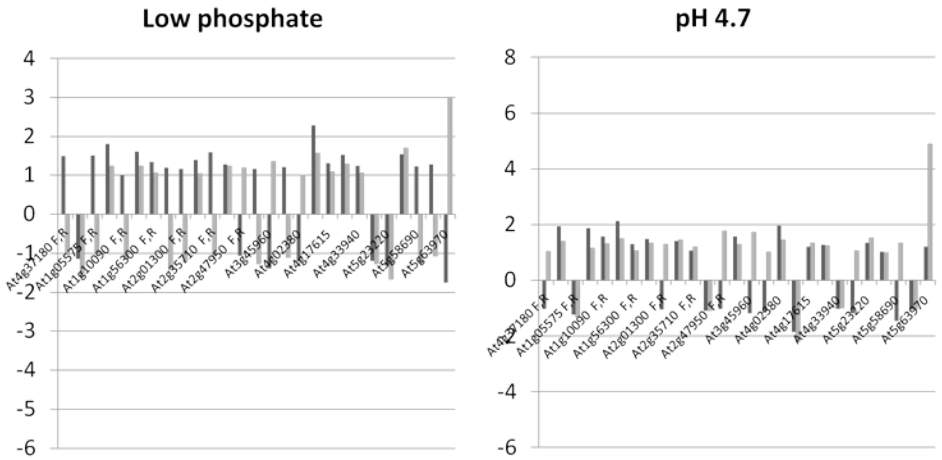

Figure 27: Normalized expression for genes in cluster 3. Graphs are representative of two biological replicates. After 3 hours on low Pi or 24 hours on acidic pH, little change in transcript abundance is observed. Note that *EXPA3* is not induced like in high salt conditions.

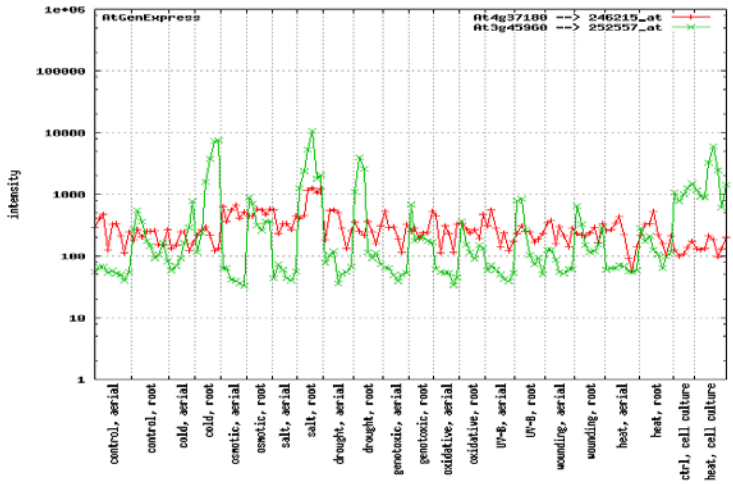

Figure 28: *SRTF1* and *EXLA3* are co-induced after salt treatment. AtGen Express data compiled from many abiotic stress expression studies reveals that co-induction of *SRTF1* (red) and *EXLA3* (green) are unique to salt treatment within roots (Kilian et al., 2007).

References

Achard P, Gusti A, Cheminant S, Alioua M, Dhondt S, Coppens F, Beemster GT, Genschik P. (2009). Gibberellin signaling controls cell proliferation rate in Arabidopsis. Current Biology **14**: 1188-93.

Alonso JM, Stepanova AN, Leisse TJ, Kim CJ, Chen H, Shinn P, Stevenson DK, Zimmerman J, Barajas P, Cheuk R, Gadrinab C, Heller C, Jeske A, Koesema E, Meyers CC, Parker H, Prednis L, Ansari Y, Choy N, Deen H, Geralt M, Hazari N, Hom E, Karnes M, Mulholland C, Ndubaku R, Schmidt I, Guzman P, Aguilar-Henonin L, Schmid M, Weigel D, Carter DE, Marchand T, Risseeuw E, Brogden D, Zeko A, Crosby WL, Berry CC, Ecker JR. (2003). Genome-wide insertional mutagenesis of Arabidopsis thaliana. Science **301(5633):** 653-7.

Bari R, Datt Pant B, Stitt M, Scheible WR. (2006). PHO2, microRNA399, and PHR1 define a phosphate-signaling pathway in plants. Plant Physiology **141**(3): 988-99.

Bayle V, Arrighi JF, Creff A, Nespoulous C, Vialaret J, Rossignol M, Gonzalez E, Paz-Ares J, Nussaume L. (2011). Arabidopsi thaliana high-affinity phosphate transporters exhibit multiple levels o posttranslational regulation. Plant Cell **23(4)**: 1523-35.

Benfey P and Scheres B. (2000). Root Development. Current Biology **10(22)**: R813-5.

Benková E, Michniewicz M, Sauer M, Teichmann T, Seifertová D, Jürgens G, Friml J. (2003). Local, efflux-dependent auxin gradients as a common module for plant organ formation. Cell **115(5)**: 591-602.

Bernhardt C, Lee MM, Gonzalez A, Zhang F, Lloyd A, Schiefelbein J. (2003). The bHLH genes GLABRA3 (GL3) and ENHANCER OF GLABRA3 (EGL3) specify epidermal cell fate in the Arabidopsis root. Development **130(26)**: 6431-9.

Birnbaum K, Jung JW, Wang JY, Lambert GM, Hirst JA, Galbraith DW, Benfey PN. (2005). Cell type-specific expression profiling in plants via cell sorting of protoplasts from fluorescent reporter lines. Nature Methods **2(8)**: 615-9.

Bishopp A, Help H, Helariutta Y. (2009). Cytokinin signaling during root development. International Reviews in Cell and Molecular Biology **276**: 1-48.

Bishopp A, Lehesranta S, Vatén A, Help H, El-Showk S, Scheres B, Helariutta K, Mähönen AP, Sakakibara H, Helariutta Y. (2011). Phloem-transported cytokinin regulates polar auxin transport and maintains vascular pattern in the root meristem. Current Biology **21(11)**: 927-32.

Bishopp A, Help H, El-Showk S, Weijers D, Scheres B, Friml J, Benková E, Mähönen AP, Helariutta Y. (2011). A mutually inhibitory interaction between auxin and cytokinin specifies vascular pattern in roots. Current Biology **21(11)**: 917-26.

Blilou I, Xu J, Wildwater M, Willemsen V, Paponov I, Friml J, Heidstra R, Aida M, Palme K, Scheres B. (2005). The PIN auxin efflux facilitator network controls growth and patternging in Arabidopsis roots. Nature **433(7021)**: 39-44.

Bonke M, Thitamadee S, Mähönen AP, Hauser MT, Helariutta Y. (2003). APL regulates vascular tissue identity in Arabidopsis. Nature **426(6963)**: 181-6.

Brady SM, Orlando DA, Lee JY, Wang JY, Koch J, Dinneny JR, Mace D, Ohler U, Benfey PN. (2007). A high-resolution root spatiotemporal map reveals dominant expression patterns. Science **318(5851)**: 801-6.

Busch W, Moore BT, Martsberger B, Mace DL, Twigg RW, Jung J, Pruteanu-Malinici I, Kennedy SJ, Fricke GK, Clark RL, Ohler U, Benfey PN. (2012). A microfluidic device and computational platform for high-throughput live imaging of gene expression. Nature Methods **9(11)**: 1101-6

Bustos R, Castrillo G, Linhares F, Puga MI, Rubio V, Pérez-Pérez J, Solano R, Leyva A, Paz-Ares J. (2010). A central regulatory system largely controls transcriptional activation and repression responses to phosphate starvation in Arabidopsis. PLoS Genetics **6(9).**

Carlsbecker A, Lee JY, Roberts CJ, Dettmer J, Lehesranta S, Zhou J, Lindgren O, Moreno-Risueno MA, Vatén A, Thitamadee S, Campilho A, Sebastian J, Bowman JL, Helariutta Y, Benfey PN. (2010). Cell signaling by microRNA165/5 directs gene dose-dependent root cell fate. Nature **465(7296)**: 316-21.

Cederholm H, Iyer-Pascuzzi A, Benfey P. (2012). Patterning the primary root in Arabidopsis. WIREs Developmental Biology DOI: 10.1002/wdev.49.

Chiou TJ, Aung K, Lin SI, Wu CC, Chiang SF, Su CL. (2006). Regulation of phosphate homeostasis by microRNA in Arabidopsis. Plant Cell **18(2)**: 412-21.

Cui H, Levesque MP, Vernoux T, Jung JW, Paquette AJ, Gallagher KL, Wang JY, Blilou I, Scheres B, Benfey PN. (2007). An evolutionarily conserved mechanism delimiting SHR movement defines a single layer of endodermis in plants. Science **316(5823):** 421-5.

Dello Ioio R, Linhares FS, Scacchi E, Casamitjana-Martinez E, Heidstra R, Costantino P, Sabatini S. (2007). Cytokinins determine Arabidopsis root-meristem size by controlling cell differentiation. Current Biology **17(8):** 678-82.

Dello Ioio R, Nakamura K, Moubayidin L, Perilli S, Taniguchi M, Morita MT, Aoyama T, Costantino P, Sabatini S. (2008). A genetic framework for the control of cell division and differentiation in the root meristem. Science **322(5906):** 1380-4.

Di Laurenzio L, Wysocka-Diller J, Malamy JE, Pysh L, Helariutta Y, Freshour G, Hahn MG, Feldmann KA, Benfey PN. (1996). The SCARECROW gene regulates an asymmetric cell division that is essential for generating the radial organization of the Arabidopsis root. Cell **86(3):** 423-33.

Dinneny JR, Long TA, Wang JY, Jung JW, Mace D, Pointer S, Barron C, Brady SM, Schiefelbein J, Benfey PN. (2008). Cell identity mediates the response of Arabidopsis roots to abiotic stress. Science **320(5878):** 942-5.

Dolan L, Janmaat K, Willemsen V, Linstead P, Poethig S, Roberts K, Scheres B. (1993). Cellular organization of the Arbidopsis thaliana root. Development **119(1):** 71-84.

Feraru E, Friml J. (2008). PIN polar targeting. Plant Physiology **147(4):** 1553-9.

Friml J, Benková E, Blilou I, Wisniewska J, Hamann T, Ljung K, Woody S, Sandberg G, Scheres B, Jürgens G, Palme K. (2002). AtPIN4 mediates sink-driven auxin gradients and root patterning in Arabidopsis. Cell **108(5):** 661-73.

Friml J, Yang X, Michniewicz M, Weijers D, Quint A, Tietz O, Benjamins R, Ouwerkerk PB, Ljung K, Sandberg G, Hooykaas PJ, Palme K, Offringa R. (2004). A PINOID-dependent binary switch in apical-basal PIN polar targeting directs auxin efflux. Science **306(5697):** 862-5.

Galinha C, Hofhuis H, Luijten M, Willemsen V, Blilou I, Heidstra R, Scheres B. (2007). PLETHORA proteins as dose-dependent master regulators of Arabidopsis root development. Nature **449(7165):** 1053-7.

Gonzalez E, Solano R, Rubio V, Leyva A, Paz-Ares J. (2005). PHOSPHATE TRANSPORTER TRAFFIC FACILITATOR1 Is a Plant-Specific SEC12-Related Protein That Enables the Endoplasmic Reticulum Exit of a High-Affinity Phosphate Transporter in Arabidopsis. The Plant Cell **17(12):** 3500-12.

Grieneisen VA, Xu J, Marée AF, Hogeweg P, Scheres B. (2007). Auxin transport is sufficient to generate a maximum and gradient guiding root growth. Nature **449(7165):** 1008-13.

Hamburger D, Rezzonico E, MacDonald-Comber Petétot J, Somerville C,Poirier Y. (2002). Identification and characterization of the Arabidopsis PHO1 gene involved in phosphate loading to the xylem. Plant Cell **14(4):** 889-902.

Hammond JP, Bennett MJ, Bowen HC, Broadley MR, Eastwood DC, May ST, Rahn C, Swarup R, Woolaway KE, White PJ. (2003). Changes in gene expression in Arabidopsis shoots during phosphate starvation and the potential for developing smart plants. Plant Physiology **132(2):** 578-96.

Hassan H, Scheres B, Blilou I. (2010). JACKDAW controls epidermal patterning in the Arabidopsis root meristem through a non-cell-autonomous mechanism. Development **137(9):** 1523-9.

Heidstra R, Welch D, Scheres B. (2004). Mosaic analyses using marked activation and deletion clones dissect Arabidopsis SCARECROW action in asymmetric cell division. Genes and Development **18(16):** 1964-9.

Helariutta Y, Fukaki H, Wysocka-Diller J, Nakajima K, Jung J, Sena G, Hauser MT, Benfey PN. (2000). The SHORT-ROOT gene controls radial patterning of the Arabidopsis root through radial signaling. Cell 101(5): 555-67.

Hinsinger P. (2001). Bioavailability of soil inorganic P in the rhizosphere as affected by root-induced chemical changes. Plant Soil **237**: 173-195.

Hürlimann HC, Pinson B, Stadler-Waibel M, Zeeman SC, Freimoser FM. (2009). The SPX domain of the yeast low-affinity phosphate transporter Pho90 regulates transport activity. EMBO Reports **10(9):** 1003-8.

Iyer-Pascuzzi AS, Jackson T, Cui H, Petricka JJ, Busch W, Tsukagoshi H, Benfey PN. (2011). Cell identity regulators link development and stress responses in the Arabidopsis root. Developmental Cell **21(4):** 770-82.

Katari MS, Nowicki SD, Aceituno FF, Nero D, Kelfer J, Thompson LP, Cabello JM, Davidson RS, Goldberg AP, Shasha DE, Coruzzi GM, and Gutierrez RA. (2010) VirtualPlant: A software platform to support Systems Biology research. Plant Physiology **152(2):** 500-15.

Kilian J, Whitehead D, Horak J, Wanke D, Weinl S, Batistic O, D'Angelo C, Bornberg-Bauer E, Kudla J, Harter K. (2007). The AtGenExpress global stress expression data set: protocols, evaluation and model data analysis of UV-B light, drought and cold stress responses. Plant Journal **50(2):** 347-63.

Koizumi K, Gallagher K. (2013). Identification of SHRUBBY, a SHORT-ROOT and SCARECROW interacting protein that controls root growth and radial patterning. Development **140(6):** 1292-300.

Koshino-Kimura Y, Wada T, Tachibana T, Tsugeki R, Ishiguro S, Okada K. (2005). Regulation of CAPRICE transcription by MYB proteins for root epidermis differentiation in Arabidopsis. Plant Cell Physiology **46(6):** 817-26.

Kubo M, Udagawa M, Nishikubo N, Horiguchi G, Yamaguchi M, Ito J, Mimura T, Fukuda H, Demura T. (2005). Transcription switches for protoxylem and metaxylem vessel formation. Genes and Development **19(16):** 1855-60.

Kurata T, Ishida T, Kawabata-Awai C, Noguchi M, Hattori S, Sano R, Nagasaka R, Tominaga R, Koshino-Kimura Y, Kato T, Sato S, Tabata S, Okada K, Wada T. (2005). Cell-to-cell movement of the CAPRICE protein in Arabidopsis root epidermal cell differentiation. Development **132(4):** 5387-98.

Kirik V, Simon M, Huelskamp M, Schiefelbein J. (2004). The ENHANCER OF TRY AND CPC1 gene acts redundantly with TRIPTYCHON and CAPRICE in trichome and root hair cell patterning in Arabidopsis. Developmental Biology **268(2):** 506-13.

Kwak SH, Shen R, Schiefelbein J. (2005). Positional signaling mediated by a receptor-like kinase in Arabidopsis. Science **307(5712):** 1111-3.

Kwak SH, Schiefelbein J. (2007). The role of the SCRAMBLED receptor-like kinase in patterning the Arabidopsis root epidermis. Developmental Biology **302(1):** 118-31.

Kwak SH, Schiefelbein J. (2008). A feedback mechanism controlling SCRAMBLED receptor accumulation and cell-type pattern in Arabidopsis. Current Biology **18(24):** 1949-54.

Lee M and Schiefelbein J. (1999). WEREWOLF, a MYB-related protein in Arabidopsis, is a position-dependent regulator of epidermal cell patterning. Cell **99(5):** 473-83.

Lee MM, Schiefelbein J. (2002). Cell pattern in the Arabidopsis root epidermis determined by lateral inhibition with feedback. Plant Cell 14(3): 611-18.

Levesque MP, Vernoux T, Busch W, Cui H, Wang JY, Blilou I, Hassan H, Nakajima K, Matsumoto N, Lohmann JU, Scheres B, Benfey PN. (2006). Whole-genome analysis of the SHORT-ROOT development pathway in Arabidopsis. PLoS Biology **4(5):** e143.

Li D, Zhu H, Liu K, Liu X, Leggewie G, Udvardi M, Wang D. (2002). Purple acid phosphatases of Arabidopsis thaliana. Comparative analysis and differential regulation by phosphate deprivation. Journal of Biological Chemistry **277(31):** 27772-81.

Liu TY, Huang TK, Tseng CY, Lai YS, Lin SI, Lin WY, Chen JW, Chiou TJ. (2012). PHO2-dependent degradation of PHO1 modulates phosphate homeostasis in Arabidopsis. Plant Cell **24(5):** 2168-83.

López-Bucio J, Hernández-Abreu E, Sánchez-Calderón L, Nieto-Jacobo MF, Simpson J, Herrera-Estrella L. (2002). Phosphate availability alters architecture and causes changes in hormone sensitivity in the Arabidopsis root system. Plant Physiology **129(1):** 244-56.

Ma Z, Bielenberg DG, Brown KM, Lynch JP. (2001) Regulation of root hair density by phosphorus availability in *Arabidopsis thaliana*. Plant Cell and the Environment **24**: 459–67.

Mähönen AP, Bonke M, Kauppinen L, Riikonen M, Benfey PN, Helariutta Y. (2000). A novel two-component hybrid molecule regulates vascular morpholgenesis of the Arabidopsis root. Genes and Development **14(23):** 2983-43.

Mähönen AP, Higuchi M, Törmäkangas K, Miyawaki K, Pischke MS, Sussman MR, Helariutta Y, Kakimoto T. (2006) Cytokinins regulate a bidirectional phosphorelay network in Arabidopsis. Current Biology **16(11):** 1116-22.

Martín AC, del Pozo JC, Iglesias J, Rubio V, Solano R, de La Peña A, Leyva A, Paz-Ares J. (2000). Influence of cytokinins on the expression of phosphate starvation responsive genes in Arabidopsis. Plant Journal **24(5):** 559-67.

Matsuzaki, Y., Ogawa-Ohnishi, M., Mori, A., Matsubayashi, Y. (2010). Secreted peptide signals required for maintenance of root stem cell niche in Arabidopsis. Science **329(5995):** 1065-7.

Miller SS, Liu J, Allan DL, Menzhuber CJ, Fedorova M, Vance CP. (2001). Molecular control of acid phosphatase secretion into the rhizosphere of proteoid roots from phosphorus-stressed white lupin. Plant Physiology **127(2):** 594-606.

Misson J, Thibaud MC, Bechtold N, Raghothama K, Nussaume L. (2004). Transcriptional regulation and functional properties of Arabidopsis Pht1;4 a high affinity transporter contributing greatly to phosphate uptake in phosphate deprived plants. Plant Molecular Biology **55(5):** 727-41.

Misson J, Raghothama KG, Jain A, Jouhet J, Block MA, Bligny R, Ortet P, Creff A, Somerville S, Rolland N, Doumas P, Nacry P, Herrerra-Estrella L, Nussaume L, Thibaud MC. (2005). A genome-wide transcriptional analysis using Arabidopsis thaliana Affymetrix gene chips determined plant responses to phosphate deprivation. Proceedings of the National Academy of the Sciences **102(33):** 11934-9.

Moubayidin L, Perilli S, Dello Ioio R, Di Mambro R, Costantino P, Sabatini S. (2010). The rate of cell differentiation controls the Arabidopsis root meristem growth phase. Current Biology **20(12):** 1138-43.

Müller A, Guan C, Gälweiler L, Tänzler P, Huijser P, Marchant A, Parry G, Bennett M, Wisman E, Palme K. (1998). AtPIN2 defines a locus of **Arabidopsis** for root gravitropism control. EMBO **17(23):** 6903-11.

Müller M, Schmidt W. (2004). Environmentally induced plasticity of root hair development in Arabidopsis. Plant Physiology **134(1):** 409-19.

Müller R, Morant M, Jarmer H, Nilsson L, Nielsen TH. (2007). Genome-wide analysis of the Arabidopsis leaf transcriptome reveals interaction of phosphate and sugar metabolism. Plant Physiology **143(1):** 156-71.

Miura K, Rus A, Sharkhuu A, Yokoi S, Karthikeyan AS, Raghothama KG, Baek D, Koo YD, Jin JB, Bressan RA, Yun DJ,Hasegawa PM. (2005). The Arabidopsis SUMO E3 ligase SIZ1 controls phosphate deficiency responses. PNAS **102(21):** 7760-5.

Nakajima K, Sena G, Nawy T, Benfey PN. (2001). Intercellular movement of the putative transcription factor SHR in root patterning. Nature **413(6853):** 307-11.

National Agricultural Statistics Service, USDA. (2012). Report on agricultural prices.

Ohashi Y, Oka A, Rodrigues-Pousada R, Possenti M, Ruberti I, Morelli G, Aoyama T. (2003). Modulation of phospholipid signaling by GLABRA2 in root-hair pattern formation. Science **300(5624):** 1427-30.

Ohashi-Ito K, Bergmann DC. (2007). Regulation of the Arabidopsis root vascular initial population by LONESOME HIGHWAY. Development **134(16):** 2959-68.

Okumura S, Mitsukawa N, Shirano Y, Shibata D. (1998). Phosphate transporter gene family of **Arabidopsis** thaliana. DNA Research **5(5):** 261-9.

Ortega-Martínez O, Pernas M, Carol RJ, Dolan L. (2007). Ethylene modulates stem cell division in the Arabidopsis thaliana root. Science **17(5837**): 507-10.

Parizot B, Laplaze L, Ricaud L, Boucheron-Dubuisson E, Bayle V, Bonke M, De Smet I, Poethig SR, Helariutta Y, Haseloff J, Chriqui D, Beeckman T, Nussaume L. (2008). Diarch symmetry of the vascular bundle in Arabidopsis root encompasses the pericycle and is reflected in distich lateral root initiation. Plant Physiology **146(1):** 140-8.

Patel, K.S., Thomas, B.E., and McKnight, T.D. (1998). Phosphate starvation induced expression of a purple acid phosphatase gene from Arabidopsis. The 9th Annual Conference on Arabidopsis Research (501708435).

Payne CT, Zhang F, Lloyd AM. (2000). GL3 encodes a bHLH protein that regulates trichome development in arabidopsisthrough interaction with GL1 and TTG1. Genetics **156(3**): 1349-62.

Prigge MJ, Otsuga D, Alonso JM, Ecker JR, Drews GN, Clark SE. (2005). Class III homeodomain-leucine zipper gene family members have overlapping, antagonistic, and distinct roles in Arabidopsis development. Plant Cell **17(1):** 61-76.

Pruteanu-Malinici I, Mace DL, Ohler U. (2011). Automatic annotation of spatial expression patterns via sparse Bayesian factor models. PLoS Computational Biology **7(7):** e1002098.

Remy E, Cabrito TR, Batista RA, Teixeira MC, Sá-Correia I, Duque P. (2012). The Pht1;9 and Pht1;8 transporters mediate inorganic phosphate acquisition by the Arabidopsis thaliana root during phosphorus starvation. New Phytologist **195(2):** 356-71.

Ruzicka K, Simásková M, Duclercq J, Petrásek J, Zazímalová E, Simon S, Friml J, Van Montagu MC, Benková E. (2009). Cytokinin regulates root meristem activity via modulation of the polar auxin transport. PNAS **106(11):** 4284-9.

Ryu KH, Kang YH, Park YH, Hwang I, Schiefelbein J, Lee MM. (2005). The WEREWOLF MYB protein directly regulates CAPRICE transcription during cell fate specification in the Arabidopsis root epidermis. Development **132(21):** 4765-75.

Sabatini S, Heidstra R, Wildwater M, Scheres B. (2003). SCARECROW is involved in positioning the stem cell niche in the Arabidopsisroot meristem. Genes and Development **17(3):** 354-8.

Schiefelbein J, Kwak SH, Wieckowski Y, Barron C, Bruex A. (2009). The gene regulatory network for root epidermal cell-type pattern formation in Arabidopsis. Journal of Experimental Biology **60(5):** 1515-21.

Schellmann S, Schnittger A, Kirik V, Wada T, Okada K, Beermann A, Thumfahrt J, Jürgens G, Hülskamp M. (2002). TRIPTYCHON and CAPRICE mediate lateral inhibition during trichome and root hair patterning in Arabidopsis. EMBO Journal **21(19):** 5036-46.

Schellmann S, Hülskamp M, Uhrig J. (2007). Epidermal pattern formation in the root and shoot of Arabidopsis. Biochemical Society Transactions **35(Pt 1):** 146-8.

Scheres B. (2007). Stem-cell niches: nursery rhymes across kingdoms. Nature Reviews Molecular Cell Biology **8(5):** 345-54.

Simon M, Lee MM, Lin Y, Gish L, Schiefelbein J. (2007). Distinct and overlapping roles of single-repeat MYB genes in root epidermal patterning. Developmental Biology **311(2):** 566-78.

Smith ZR, Long JA. (2010). Control of Arabidopsis apical-basal embryo polarity by antagonistic transcription factors. Nature **464(7287):** 423-6.

Smith AP, Nagarajan VK, Raghothama KG. (2011). Arabidopsis Pht1;5 plays an integral role in phosphate homeostasis. Plant Signaling Behavior **6(11):** 1676-8.

Sozzani R, Cui H, Moreno-Risueno MA, Busch W, Van Norman JM, Vernoux T, Brady SM, Dewitte W, Murray JA, Benfey PN. (2010). Spatiotemporal regulation of cell-cycle genes by SHORTROOT links patterning and growth. Nature **466(7302):** 128-32.

Stepanova AN, Yun J, Likhacheva AV, Alonso JM. (2007). Multilevel interactions between ethylene and auxin in Arabidopsis roots. Plant Cell **19(7):** 2169-85.

Svistoonoff S, Creff A, Reymond M, Sigoillot-Claude C, Ricaud L, Blanchet A, Nussaume L, Desnos T. (2007). Root tip contact with low-phosphate media reprograms plant root architecture. Nature Genetics **39(6):** 792-6.

Swarup R, Perry P, Hagenbeek D, Van Der Straeten D, Beemster GT, Sandberg G, Bhalerao R, Ljung K, Bennett MJ. (2007). Ethylene upregulates auxin biosynthesis in Arabidopsis seedlings to enhance inhibition of root cell elongation. Plant Cell **19(7):** 2186-96.

Ticconi CA, Lucero RD, Sakhonwasee S, Adamson AW, Creff A, Nussaume L, Desnos T, Abel S. (2009). ER-resident proteins PDR2 and LPR1 mediate the developmental response of root meristems to phosphate availability. PNAS **106(33):** 14174-9.

Ubeda-Tomás S, Swarup R, Coates J, Swarup K, Laplaze L, Beemster GT, Hedden P, Bhalerao R, Bennett MJ. (2008). Root growth in Arabidopsis requires gibberellin/DELLA signalling in the endodermis. Nature Cell Biology **10(5):** 625-8.

Ubeda-Tomás S, Federici F, Casimiro I, Beemster GT, Bhalerao R, Swarup R, Doerner P, Haseloff J, Bennett MJ. (2009). Gibberellin signaling in the endodermis controls Arabidopsis root meristem size. Current Biology **19(14):** 1194-9.

Wada T, Tachibana T, Shimura Y, Okada K. (1997). Epidermal cell differentiation in Arabidopsis determined by a Myb homolog, CPC. Science **277(5329):** 1113-6.

Wang, Y.,Ribot, C.,Rezzonico, E.,Poirier, Y. (2004). Structure and Expression Profile of the Arabidopsis PHO1 Gene Family Indicates a Broad Role in Inorganic Phosphate Homeostasis. Plant Physiology **135(1):** 400-11.

Wang L, Li Z, Qian W, Guo W, Gao X, Huang L, Wang H, Zhu H, Wu JW,Wang D, Liu D. (2011). The Arabidopsis purple acid phosphatase AtPAP10 is predominantly associated with the root surface and plays an important role in plant tolerance to phosphate limitation. Plant Physiology **157(3):** 1283-99.

Webb M, Jouannic S, Foreman J, Linstead P, Dolan L. (2002). Cell specification in the Arabidopsis root epidermis requires the activity of ECTOPIC ROOT HAIR 3--a katanin-p60 protein. Development **129(1):** 123-31.

Welch D, Hassan H, Blilou I, Immink R, Heidstra R, Scheres B. (2007). Arabidopsis JACKDAW and MAGPIE zinc finger proteins delimit asymmetric cell division and stabilize tissue boundaries by restricting SHORT-ROOT action. Genes and Development **21(17):** 2196-204.

Wu P, Ma L, Hou X, Wang M, Wu Y, Liu F, Deng XW. (2003). Phosphate starvation triggers distinct alterations of genome expression inArabidopsis roots and leaves. Plant Physiology **132(3):** 1260-71.

Xia G, Ramachandran S, Hong Y, Chan YS, Simanis V, Chua NH. (1996). Identification of plant cytoskeletal, cell cycle-related and polarity-related proteins using Schizosaccharomyces pombe. Plant Journal **10(4):** 761-9.

Yadav RK, Fulton L, Batoux M, Schneitz K. (2008). The Arabidopsis receptor-like kinase STRUBBELIG mediates inter-cell-layer signaling during floral development. Developmental Biology **323(2):** 261-70.

Yamaguchi M, Kubo M, Fukuda H, Demura T. (2008). Vascular-related NAC-DOMAIN7 is involved in the differentiation of all types of xylem vessels in Arabidopsis roots and shoots. Plant Journal **55(4):** 652-64.

Yamaguchi M, Goué N, Igarashi H, Ohtani M, Nakano Y, Mortimer JC, Nishikubo N, Kubo M, Katayama Y, Kakegawa K, Dupree P, Demura T. (2010). VASCULAR-RELATED NAC-DOMAIN6 and VASCULAR-RELATED NAC-DOMAIN7 effectively induce transdifferentiation into xylem vessel elements under control of an induction system. Plant Physiology **153(3):** 906-14.

Zhang F, Gonzalez A, Zhao M, Payne CT, Lloyd A. (2003). A network of redundant bHLH proteins functions in all TTG1-dependent pathways of Arabidopsis. Development **130(20):** 4859-69.

Zhang H, Han W, De Smet I, Talboys P, Loya R, Hassan A, Rong H, Jürgens G, Paul Knox J, Wang MH. (2010). ABA promotes quiescence of the quiescent centre and suppresses stem cell differentiation in the Arabidopsis primary root meristem. Plant Journal **64(5):** 764-74.

Biography

Born as the "caboose" of four children, Heidi spent her early life in a small town on the Olympic Peninsula called Forks, WA. After a move to the "big city" of Olympia, WA, she grew up in the suburbs with her parents and brother, and remained close with her two older sisters who are her best friends. She graduated with a Bachelor's of Science in 2004 from The Evergreen State College, and continued to develop her skills and interest in research as an Oak Ridge Institute for Science and Education Fellow. Then, she accepted a position to assist with research in the Madigan Army Medical Center Department of Clinical Investigation. Following the death of her father, Heidi applied to graduate school and moved to Durham to attend Duke as a student of Cell and Molecular Biology. During graduate school, she affiliated with the Genetics and Genomics Program and pursued questions in Plant Developmental Biology for her thesis work. She is the first author of an advanced review entitled "Patterning the Primary Root" in the journal *WIREs Developmental Biology* and will be the first author of a manuscript submitted to the journal *The Plant Cell*. Beyond the lab, she developed teaching skills within the Certificate for College Teaching Program and enjoyed mentoring middle school-aged girls in Durham through a local non-profit organization focused on introducing girls to careers in STEM-related fields. Heidi, and her soon-to-be husband Horacio, will move to Hanover, NH this summer where she will pursue post-doctoral training and he, an MBA.